2nd AMDI International ONCOLOGY & MEDICAL PHYSICS Symposium

Advancing Cancer Care, Fostering Cancer Research

ABSTRACT BOOK

Contents

Medical Physics
(Radiotherapy)

ID #1: A review of dose to extremities using conventional and automated radiopharmaceutical dispenser system

R Zainon[1], N A B Amin[1], M A Said[2]

[1]Oncological and Radiological Sciences Cluster, Advanced Medical and Dental Institute, Universiti Sains Malaysia, SAINS@BERTAM, 13200 Kepala Batas, Pulau Pinang, Malaysia; [2]Department of Nuclear Medicine, National Cancer Institute, No. 4, Jalan P7, Presint 7, 62250 Wilayah Persekutuan, Putrajaya, Malaysia.

Manual dispensing technique of radiopharmaceutical in nuclear medicine involves manual withdrawal of activity from an elution vial, from a combination of the syringe and elution vial activities, and preparation of individual radiopharmaceutical doses to patients. Commercial automated radiopharmaceutical dispensing system is available, but, the cost of the machine is very expensive. The main aim of this study is to review the radiation burden to extremities of nuclear medicine personnel during preparation and dispensing of radiopharmaceutical using manual and automated dispensing system. The manual dispensing technique is laborious, and it involves high extremity doses to nuclear medicine personnel even with the use of heavy shielded containers. Thus, nuclear medicine personnel receive radiation burden to the hands and whole-body resulting from the practice of preparation of radiopharmaceutical doses. It is reported that radiation doses to both the fingertip and finger base of nuclear medicine personnel that prepares the radiopharmaceuticals in a radionuclide dispensary are likely to receive high dose and may even exceed the dose limit if the radiation protection principle is not well implemented. Therefore, a critical analysis of the distribution of dose across the extremities of nuclear medicine personnel using both manual and automated dispensing system was performed in this study. The contribution to the dose from automated system significantly reduce the radiation dose to extremities using automated dispensing system. This review also highlights that there is an urgent need to have a system that allows a real-time calibration and withdrawal of radiopharmaceutical to reduce extremity and whole-body doses.

Contact author: rafidahzainon@usm.my

Keywords: radiopharmaceutical, dispensing technique, dose to extremities

ID #4: Improving the accuracy of dosimetric verification in pre-treatment Head-and-Neck VMAT by nonuniform nackscatter correction in the EPID.

Yasmin Md Radzi[1], Rebecca S Windle[2], D.G.Lewis[2], Emiliano Spezi[3]

[1]School of Physics, Universiti Sains Malaysia, Penang, 11800, Malaysia; [2]Physics department, Velindre Cancer Centre, Cardiff, CF14 2TL, United Kingdom; [3]School of Engineering, Cardiff University, Roath, Cardiff, CF24 3AA, United Kingdom.

The validation of the radiotherapy dose verification using an Electronic Portal Imaging Device (EPID)-based method has been widely discussed and in this presentation, we emphasized on the implementation of the commercially available Dosimetry Check (DC) system, to address the significant of nonuniform backscatter effect from the Varian aS1000 EPID arm. A backscatter correction matrix was developed by attaining the dosimetric information from segmented fields sampling on different positions around the panel imager. A corrective factor was used to correct EPID images using Matlab scripts. The corrected image was created in DICOM format and exported to DC to analyse. The feasibility of the developed correction to a clinical pre-treatment Volumetric Modulated Arc Therapy (VMAT) Head-and-Neck was investigated using DC system. The assessment included, i) improvement of the beam profiles along in-line direction, ii) pass-rate of the gamma criteria of 3%/5mm and 3%/3mm and iii) pass rate of gamma volume index. Utilising the correction, average percentage difference relative to TPS dose improved from 4.2% to 1.7%. For gamma criterion of 3%/5mm, 95% and 97% of points passing gamma at coronal and sagittal planes respectively whereas more than 85% of points passing gamma for 3%/3mm at both planes. Gamma volume index for regions of interest within the Head-and-Neck phantom also improved from 73% to 87% and from 89% to 95% for 3%/3mm and 3%/5mm gamma criteria respectively. A `proof-of-concept' of this method has shown to give benefit to clinical treatment verification techniques and effectively reduces inaccuracy associated with the affected Varian EPID arm.

Contact author: Yasmin Md Radzi; yasminradzi@usm.my

Acknowledgement: Author would like to signature a token of appreciation to grant number RUI.1001/PFIZIK/8011087 as the funder of this presentation.

Keywords: EPID dosimetry, DosimetryCheck, pre-treatment VMAT

ID #6: Dosimetric evaluation of organ at risk doses in image guided brachytherapy for cervical cancer: a single institutional experience

R. Abdullah[1,2], M.F. Mohd Sepian[1], C.S. Chiang[1], K. Gokula[2], A. Zakaria[1], M. Z. A. Aziz[3]

[1]Medical Radiation Programme, School of Health Sciences, Universiti Sains Malaysia, Kota Bharu, Kelantan, 16150, [2]Radiology and Oncology Cluster, Advanced Medical and Dental Institute, Universiti Sains Malaysia, Bertam, Penang, Postcode, Malaysia

The purpose of this study is to compare point doses recommended by International Commission on Radiation Units and Measurement (ICRU) with volumetric dose to 2cc based on dose volume histogram (DVH) analysis of organs at risk for three dimensional (3D) intracavitary brachytherapy. A retrospective study was carried out on 3 cervical cancer patients with a total of 6 fractions of CT-based high dose rate (HDR) intracavitary brachytherapy (ICBT) from December 2017 to May 2018. ICRU bladder (bICRU) and rectum (rICRU) points were defined according to ICRU Report 38 on the CT images. Post-treatment, outer wall of OARs was contoured and minimum dose to 2cc (D2cc) of the most irradiated part of the OARs was obtained from the dose-volume histogram (DVH). Total doses (external beam radiotherapy plus ICBT) were computed with ICRU point dose and D2cc and then compared. There were 2 out of 3 patients, 2 out of 3 patients, and none of patients exceeded the (GYN) GEC-ESTRO Working Group recommended tolerance doses for bladder, rectum, and sigmoid, respectively. The mean ICRU point doses and D2cc volume doses were found to be significantly different for bladder with average ratio of 1.35, but no difference was found for rectum with average ratio of 1.03.

Contact author: Reduan Abdullah; reduan@usm.my

Acknowledgement: This study was supported financially by RUI Grant (No. 1001304/CIPPT/8011001) of the Malaysian Ministry of Higher Education.

Keywords: organ at risk doses, intracavitary brachytherapy, cervical cancer

ID #7: 2D dose reconstruction of IMRT patient-specific QA based on log file information

S Mubarok[1], W E Wibowo[2], S A Pawiro[1]

[1]Department of Physics, Faculty of Mathematics and Natural Sciences, Universitas Indonesia, Depok, West Java 16424, Indonesia; [2]Department of Radiotherapy, Cipto Mangunkusumo Hospital, Jakarta, 10430, Indonesia

This study aimed to reconstruct the 2D dose distribution based on log file and use it for IMRT patient-specific QA. Log file of Varian Unique Linear Accelerator was extracted to calculate the fluence MU and then converted to 2D dose distribution using the modified Clarkson integration (MCI) method. All calculation were done using in-house software based on MATLAB version 2016a. This reconstruction using the assumption that cube water phantom was irradiated by 6 MV photon at source surface distance (SSD) 98.5 cm and depth at 1.5 cm. This 2D dose reconstruction was compared with Eclipse™ treatment planning system (TPS) calculation. The evaluation was done at isocenter point and 2D evaluation using gamma index analysis. The evaluation was separated by the split field (large IMRT field) and non-split field (small IMRT field). The isocenter dose evaluation results were 89 % and 36% data for non-split field and split field had deviation below 3 %. The gamma pass-rate results for non-split field with 2%/2 mm, 3%/3 mm and 4%/4 mm criteria were above 84%, 90% and 95% respectively. On the other hand, the gamma pass-rate results for split field with 2%/2mm, 3%/3 mm and 4%/4mm criteria were above 78%, 85% and 90% respectively. This results showed that log file information can be used to reconstruct 2D dose distribution and potentially to be used for IMRT patient-specific QA.

Contact author: sayid.mubarok@sci.ui.ac.id

Acknowledgement: This research was funded by UI Research Grant or Hibah PITTA 2018.

Keywords: log file, dose reconstruction, patient-specific QA

ID #9: Elemental decomposition and fractional probability of photon interaction in *Rhizophora* spp. bonded with soy protein particleboard

Nor Ain Rabaiee[1], Mohd Zahri Abdul Aziz[1], Abdul Aziz Tajuddin[2], Ahmad Lutfi Yusoff[3], Rokiah Hashim[4], Muhammad Fadhirul Izwan Abdul Malik[5], Reduan Abdullah[6]

[1]Advanced Medical and Dental Institute, Universiti Sains Malaysia, 13200 Bertam, Pulau Pinang, Malaysia; [2]School of Physics, Universiti Sains Malaysia, 11800 Minden, Pulau Pinang, Malaysia; [3]I Hospital Universiti Sains Malaysia, 16150 Kubang Kerian, Kelantan, Malaysia ;[4]School of Industrial Technology, Universiti Sains Malaysia, 11800 Minden, Pulau Pinang, Malaysia; [5]Science and Engineering Research Center, Universiti Sains Malaysia Engineering Campus, 14300 Nibong Tebal, Pulau Pinang, Malaysia; [6]School of Health Science, Universiti Sains Malaysia Health Campus, 16150 Kubang Kerian, Kelantan, Malaysia

Several solid water phantoms are not exactly equivalent to water (even though they were called with the similar name), as they consist of different mixtures and formulations. These materials should provide similar physicochemical properties, i.e. density and elemental composition at certain energy range, to that of the real soft tissue. Several studies have been conducted on the *Rhizophora* spp. wood and found its attenuation coefficient was similar to water. However, no similar study has yet been conducted on the *Rhizophora* spp. bonded with soy protein, as it is expected that the soy protein should improve the bonding and mechanical properties of the wood. In this work, the *Rhizophora* spp. bonded with soy protein particleboard was analysing for its elemental composition and future evaluated its probability of photon interaction using Monte Carlo simulation. The probability of photon interactions, i.e. photoelectric effect, Compton scattering and pair production, provides a comparable curve as the solid water phantom and water phantom at the energy range between 0.001 and 50.000 MeV. Meantime, the Monte Carlo simulation showed that the depth dose curves with respect to water for 6 and 10 MV photon beam were in an acceptable value with discrepancy less than 5 %. Therefore, results of this study support the comparable results on probability of photon interaction between *Rhizophora spp.* bonded with soy protein particleboard with the water.

Contact author: norainrabaiee@gmail.com

Acknowledgement: The authors would like to express their appreciation to the School of Industrial Technology, Universiti Sains Malaysia (USM); the Cluster of Oncological and Radiological Sciences, Advanced Medical and Dental Institute (AMDI); Department of Nuclear Medicine, Radiotherapy and Oncology, Hospital Universiti Sains Malaysia as well as the Science and Engineering Research Centre (SERC), Engineering Campus, USM. The authors would also like to thank the Ministry of Higher Education, Malaysia, for the research funding, i.e. the Fundamental Research Grants Scheme (FRGS) 203/CIPPT/6711341.

Keywords: mangrove wood; water equivalent phantom; Monte Carlo, photon interaction, dose distribution

ID #16: Treatment planning system dose evaluation of air-gaps for small field FFF beam irradiation

A Azzi[1], D Ryangga[2], SA Pawiro[1]

[1]Department of Physics, Faculty of Math and Natural Science, Universitas Indonesia, Depok, West Java, 16424, Indonesia; [2]Department of Radiotherapy, Pasar Minggu Regional General Hospital, South Jakarta, Jakarta, 12550, Indonesia

Many authors stated that cavities or air-gap was the main challenge of dose calculation for Head and Neck with Flattening Filter LINAC irradiation. The aim of this work was to evaluate the effect of air-gap inhomogeneity dose calculation of flattening-filter-free (FFF) small field irradiation. Monte Carlo (MC) simulation was employed to study the characteristics of FFF beam in heterogeneity region. Virtual phantoms of 0, 2, 4, 6, 8, 10, and 15 mm air-gaps were built for 1×1, 2×2, 3×3, 4×4 cm^2 6 MV FFF dose calculation. The dose ratio of air-gaps to tissue-equivalent was calculated both in Anisotropic Analytical Algorithm (AAA) and MC. In addition, the dose difference of AAA and MC were evaluated inside and below the air-gaps. We found that the dose ratio of air to tissue-equivalent tend to decrease with larger field size. This correlation was linear with a slope of -0.198±0.001 and -0.161±0.014 for both AAA and MC, respectively. On the other hand, the dose ratio beneath the air-gap was slightly field size dependent. The AAA to MC dose calculation as the impact of air-gap thickness and field size was varied from 1.57 to 5.35% after the gap. Uniquely, the dose difference was found up to 134% for 15 mm air-gap at 1×1 cm^2. The dose air to tissue-equivalent ratio decreased with smaller air gaps and larger field sizes. Dose correction for AAA calculation beneath air-gap could be ignored after the secondary buildup. However, it should be applied inside the air-gap for FFF dose calculation.

Contact author: Akbar Azzi; akbar.azzi@sci.ui.ac.id

Keywords: dose calculation, flattenning-filter-free, air-gap, Monte Carlo, small field

ID #26: Computed Tomography Room Shielding Calculation of 140 keV Photons Using Monte Carlo Simulation

M. F. Yusop[1], N. Kamarullah Ya Ali[2], S. M. Tajudin[3], H. Iwase[4,5], M. Musarudin, M. Z. Abdul Aziz[1]

[1]Oncological and Radiological Science Cluster, Advance Medical and Dental Institute, Universiti Sains Malaysia, 13200 Kepala Batas, Penang, Malaysia, [2]Department of Radiology, Hospital Universiti Sains Malaysia,, Universiti Sains Malaysia, 16150 Kubang Kerian, Kelantan, Malaysia, [3]Universiti Sultan Zainal Abidin, Faculty of Health Sciences, 21300, Kuala Nerus, Terengganu, Malaysia, [4]High Energy Accelerator Research Organization (KEK), 1-1Oho, Tsukuba, Ibaraki 305-0801, Japan [5]Department of Accelerator Sience, Graduate University for Advanced Studies (SOKENDAI), 1-1 Oho, Tsukuba, Ibaraki 305-0801, Japan, [6]School of Health Sciences, Health Campus, Universiti Sains Malaysia, 16150 Kubang Kerian, Kelantan

In recent years, Computed Tomography (CT) modality has been frequently used for the diagnosis and treatment of a diseases. With the increased request on CT procedure, radiation risk to staff will also rise. The objective of this study is to calculate radiation photon dose level in CT console room shielded with concrete and Barium plaster using Monte Carlo simulation (PHITS code). The exact size of the staff room, CT control console room and CT scanner room were modelled and simulated using the PHITS code. The source was modelled by 140 keV photons emitted isotropically in the CT room at 2-meter height from the floor. The CT console room where selected for the assessment of the radiation dose due to the highest probability for radiation workers to receive occupational exposure in this area. The findings showed that the dose level was higher at the opposite to the CT control console. The data also showed that interactions of the primary beam with the concrete floor above the CT room produces secondary radiation in the respective room. Hence, the suitable shielding materials (Aluminium, Al and Zinc, Zn) and with thickness 1 and 5 cm were introduced in the simulations. At highest dose point in CT control room 1 cm of Zinc and reduce dose by 82% compared to only 4% using 1 cm of aluminium slab.

Contact author: mr.zahri@gmail.com

Keywords: PHITS, Monte Carlo, CT control console room, Aluminium, Zinc

ID #28: Dosimetric comparisons between two and three dimensional treatments plans for prostate Cancer

Yousra Khairi Mohamed[1], Maha Hassan[2] ,Einas AbdelRahman[3], Hiba Omer[4], Esameldeen Babikir5, Abdelmoneim Suleiman[6]*

[1]College of preparatory year, Aljuf University, Skaka, Aljuf, Kingdom of Saudi Arabia, *[2]National Cancer institute,University of Cairo, Cairo Egypt*, *[3]College of preparatory year, Aljuf University, Al Qurayyat, Aljuf , Kingdom of Saudi Arabia*, *[4]College of Medicine, Deanship of preparatory year, Imam Abdulrahman Bin Faisal University, Dammam Kingdom of Saudi Arabia*, *[5]Bahrain University, College of Health Sciences, Allied Health Department.Radiologic Technology Program, Kingdom of Bahrain*, *[6]Radiology and Medical Imaging Department, College of Applied Medical Sciences, Prince Sattam bin Abdulaziz University. P.O.Box 422, Alkharj11943, Kingdom of Saudi Arabia*

This study intended to compare between two-dimensional (2D) and three-dmensional (3D) techniques for external-beam radiation treatment for prostate cancer was conducted at the National Cancer Institute, Egypt. Dose homogeneity within the target volume and doses to critical organs, organ at risk (OAR) were evaluated. CT scans of 30 patients with localized prostate cancer (T2N0M0) were acquired and transferred to the treatment planning systems ((TPS), KonRad version 2.2.23 Siemens, Malvern, PA, USA). A comparison of the two techniques was performed using isodose distributions, and dose-volume histograms. For the planning target volume (PTV) , the average (V95%, V107%) in 2D technique 90.6%, 5.7% while, for 3D technique 94.9%, 3.8 respectively. However, a better distribution of dose received by the OAR is achieved using 3D as compared to that of 2D technique, with considerable sparing of bladder, rectum and head of both femora, which received unnecessary radiation doses using 2D techniques. The discrepancy is very noticeable in the: rectum, where the average (V70, V75 and D95) in 2D technique was found to be 35.5%, 32.2%, 34% while for 3D 8.4%, 0.2%, 12% respectively; and the bladder where the average (V40, V65) in 2D technique was found to be 80.8%, 74.9% while for 3D it was 20.4%, 17% respectively. 3D planning only for prostate cancer treatment provides better target coverage and reduces the dose to the OAR and is thus more appropriate for prostate cancer therapy. Multiple 3D field, did not result in major difference in target coverage compared to the 2D techniques.

Contact author: Abdelmoneim Sulieman; abdelmoneim_a@yahoo.com

Keywords: prostate cancer; treatment planning; 2D plans; radiation risk

ID #49: Intensity threshold based segmentation method for Positron Emission Tomography (PET) images: a review

M. Tamal[1] and R. Zainon[2].

[1]Department of Biomedical Engineering, Imam AbdulRahman Bin Faisal University, Dammam, Eastern Province,1982-31441, Kingdom of Saudi Arabia, [2]Oncological and Radiological Sciences Cluster, Advanced Medical and Dental Institute, Universiti Sains Malaysia, SAINS@BERTAM, 13200 Kepala Batas, Pulau Pinang, Malaysia,

Diagnosis, treatment planning and response assessment of tumours using Positron Emission Tomography (PET) images require accurate, robust and reproducible segmentation of the tumours. Since standardized uptake value (SUV) – a normalized semiquantitative parameter that is conventionally used in PET is represented by the intensity of the PET images and related to the radiotracer uptake by the tumour and surrounding background organs or tissues, a SUV based threshold method is a natural choice to delineate the tumour from the background. However, due to low signal-to-signal ratio (SNR) and poor spatial resolution of PET camera along with the finite image sampling constraint, determining an optimum threshold value is a challenging task. The aims of this study are to review the fixed and adaptive threshold based PET image segmentation approaches utilizing a common mathematical framework and to highlight the advantages and disadvantages of these methods from the perspectives of diagnosis, treatment planning and response assessment. Several fixed threshold values have been proposed over the years ranging from 40% to 50% of the maximum SUV (SUV_{max}). It has been observed that the performance of the fixed threshold based method is very much dependent on the SNR, contrast and size of the tumour. To minimize these dependencies, different versions of the threshold based method that account for signal to background ratio and size of the tumour have been proposed. These methods are known as adaptive threshold based methods.

Keywords: intensity threshold segmentation, PET, standardized uptake value (SUV)

ID #60: A review on radiation shielding materials in nuclear medicine

Nadin Jamal AbuAlRoos[1], Rafidah Zainon[1]

[1]*Oncological and Radiological Sciences Cluster, Advanced Medical and Dental Institute – Universiti Sains Malaysia, SAINS@BERTAM, 13200 Kepala Batas, Pulau Pinang, Malaysia.*

Gamma ray is an energetic ionizing radiation that has the ability to damage living cells as it slows down and transfers its energy to the surrounding cells. Shielding is essential in protection against gamma ray hazards. Radiation shielding materials become very serious issue, researchers are continuously looking for sustainable shielding material. Different shielding materials have been produced to safeguard the human and the environment from destructive impact of radiation throughout the past decades.

A good perceiving of gamma ray interaction with matter is the first key to find shielding material with appropriate physical properties. Materials with high atomic number and high-density elements imposed high probability of interactions and larger energy transfer with gamma rays considered as a good choice for effective gamma shields. Heavy materials known to have high ability in attenuation of gamma rays which is the most important characteristic of a material protection.

The high atomic number and high-density materials such as lead, steel, tungsten and concrete provide best effective shielding against Gamma-ray with taking into consideration the toxicity of lead and the need of finding alternative material to replace it.

Numerous experimental and theoretical works have been performed on radiation shielding. In this paper, the recent developments of materials used as gamma radiation shielding in nuclear medicine applications are reviewed.

Contact author: Dr. Rafidah Zainon, rafidahzainon@usm.my

Keywords: Ionising radiation, Gamma ray, shielding materials.

ID #64: Fabrication of Anthropomorphic Tissue-equivalent Thyroid-neck Phantom use in Nuclear Medicine

Noorfatin Aida B. A. [1], R. Zainon[2]

[1]Advanced Medical and Dental Institute, Universiti Sains Malaysia, Bertam 13200 ,Kepala Batas, Pulau Pinang, Malaysia. [2]School of Physics, Universiti Sains Malaysia, 11800 Minden, Pulau Pinang, Malaysia.

The aim of this study was to fabricate anthropomorphic thyroid-neck phantom used in nuclear medicine. The phantom can be used for internal dosimetric studies and single-photon emission computed tomography (SPECT) imaging. The main structures of this fabricated anthropomorphic phantom was it included the neck shape, thyroid, trachea, oesophagus, cervical bone and spinal canal mimicking structure with optically stimulated luminescence dosimetry (OSLD) slots. All structures of this phantom are were fabricated using tissue-equivalent material of paraffin wax and sodium chloride (NaCl) compound. Technetium-99m (Tc^{99m}) with an activity of 0.3 mCi and 2.0 mCi were administrated into the thyroid part and correspond structures of neck and spinal canal of the fabricated phantom which imitate the background radiation when radiophramaceutical administrated into human body. The OSLDs were inserted into the thyroid, spinal canal, trachea and eosophagus parts for dosimetry purposes while the images of these anthropomorphic tissue-equivalent thyroid-neck phantom were obtained using SPECT imaging. From the experiment using fabricated phantom, the effective dose measured at thyroid, oesophagus, trachea and spinal canal parts of phantom are 0.455mSv, 0.393 mSv, 0.427 mSv and 0.373 mSv respectively. The percentage difference between average effective dose of thyroid phantom calculated and ICRP report 53 is 31%. The fabricated anthropormorphic thyroid-neck phantom can be future use to study of radiation dosimetry under conditions very similar to those in patient. Internal dose radiation can be analyse for nuclear medicine procedures of thyroid using the fabricated phantom and dosimeters.

Contact author: PresentingAuthor; noorfatinaida@gmail.com

Acknowledgement: The author would like to acknowledge Nuclear Medicine Unit, Advanced Medical and Dental Institute in providing the radiopharmaceutical source and SPECT imaging.

.

Keywords: anthropomorphic phantom, tissue equivalent material, dosimetry, $Tc^{99m,}$ nuclear medicine.

ID #65: Advanced thermoluminescence dosimetric characterization of fabricated Ge-doped optical fibres (FGDOF) for electron beams dosimetry

Z Zakaria[1, 3], M Z Abdul Aziz[2], N Mohd Noor[1]

[1]Department of Imaging, Faculty of Medicine and Health Sciences, Universiti Putra Malaysia, 43400 UPM Serdang, Selangor, Malaysia, *[2]Oncological and Radiological Sciences Cluster, Institut Perubatan & Pergigian (IPPT), Universiti Sains Malaysia (USM), 13200, Bertam, Penang, Malaysia*, *[3]Universiti Kuala Lumpur British Malaysian Institute (UniKL BMI), Bt 8 Jalan Sg Pusu, 53100 Gombak, Selangor, Malaysia*

This work was investigated on an advanced dosimetric characteristic of fabricated Ge-doped optical fibres (FGDOF) for electron beams dosimetry in term of percentage depth dose (PDD) curves besides of basic characteristics of sensitivity, dose linearity, dose rates dependences, field sizes dependences and fading. The fibres used were different in shapes, cross-section dimensions and germanium concentrations. Responses of fibres are compared with commercial fibres, ionization chamber (IC) and Gafchromic^{TM} EBT3 films. All the fibres were irradiated using 6-, 9- and 12 MeV electron energies, 100 cm focus to sample distance (FSD) and 10 x 10 cm^2 field size to the depth of dose maximum at the Royal Surrey County Hospital, England. The dose rates employed ranges from 100 up to 600 cGy/min and field size ranges from 6 x 6 cm^2 to 25 x 25 cm^2 respectively at fixed 9 MeV electron's energy. For PDD curves, the fibres, IC and films were placed at the depth ranges from 0cm to 10cm. The water-to-air stopping power ratios and the fluence correction factors, *P*fl were required in determining PDD curves when using ionization chamber. Thermoluminescence (TL) yields for the fibres showed high linearity ($R^2 > 0.99$) compared to commercial fibres. A weak dependence showed on dose rates and field sizes dependences to within 5% for all fibres. The highest sensitivity and minimum TL fading for up to three months were reported for a 2.3 mol% flat fibre (FF). Differences of up to 3% were identified between the PDDs measured using IC and FGDOF.

Contact author: noramaliza@upm.edu.my

Acknowledgement: The authors warmly thank the staff of Medical Physics Department at the Royal Surrey County Hospital for the irradiations assistance. Universiti Putra Malaysia (UPM) is gratefully acknowledged for financial support through Putra grant (project no: 9615500).

Keywords: thermoluminescence, depth of dose maximum, Ge-doped optical fibres

ID #67: Optical fiber scintillators for pulse-by-pulse measurement of radiation doses in IMRT treatment plans

H.T. Zubair[1], Hafiz M Zin[2], A. Oresegun[1], G.T. Louay[1], H.A. Abdul-Rashid[1], Z. Yusoff[1], D.A. Bradley[3, 4]

[1]Fibre Optics Research Centre, Faculty of Engineering, Multimedia University, Jalan Multimedia 63100, Cyberjaya, Malaysia.[2]Advanced Medical and Dental Institute (AMDI), Universiti Sains Malaysia, Penang, Malaysia. [3]Centre for Radiation Sciences, Sunway University, 46150 PJ, Malaysia, [4]Department of Physics, University of Surrey, Guildford, GU2 7XH, UK

Specialised treatment modalities in radiation therapy such as Intensity Modulated Radiation Therapy (IMRT) demand for radiation sensors with high spatial resolution and fast response. More than 60% of cancer patients receive a form of radiation therapy to manage the tumour. Scintillation dosimetry utilizing fibre optic coupling arrangement has emerged as one of the most promising candidates for small-field ionizing radiation dose measurements. Recent advances have also explored the possibilities of in vivo dose measurements using similar apparatus. In this study, phosphorus-doped silica optical fibre scintillators, fabricated in-house using Modified Chemical Vapour Deposition (MCVD) technique, have been developed in conjunction with a fibre optic coupled radioluminescence (RL) signal acquisition system. Together, they make a real-time, remote dosimetry system for use in megavoltage X-ray environment (radiotherapy range). The 'real-time' feature can be extended to pulse-by-pulse measurements of linac beams, where each pulse ideally delivers ~0.23 mGy at 6MV, and ~0.45 mGy at 10MV. This feature has significant value, when treatment plans involve variable dose rates. Feasibility of pulse-by-pulse measurements of linac beams using P-doped silica optical fibre scintillators (of varying dimensions and composition) has been experimentally investigated in IMRT treatment plans achieving a Radioluminescence (RL) response with precision level ±3% satisfying the International Atomic Energy Agency (IAEA) TRS-98 specifications.

Contact author: H.T. Zubair; zubair.tarif@gmail.com

Keywords: Radioluminescence, Time-resolved Dosimetry, Optical Fibre Scintillator

Medical Physics
(Imaging)

ID #10: Dose Assessment of 4- and 16-slices Multi-Detector Computed Tomography (MDCT) Scans

R. S. Omar[1], S. Hashim[1], S. K. Ghoshal[1], N. D. Shariff[2]

[1,]Universiti Teknologi Malaysia, Skudai, Johor, 81310, Malaysia; [2]Hospital Sultanah Aminah, Johor Bahru, 80100, Malaysia

This paper reports the performance of x-ray generator and CT dosimetry in 4- and 16-slices Multi-Detector Computed Tomography (MDCT) scanners in axial mode scanning. 2 types of CT scanner were evaluated; 16-slices Siemen Somatom Emotion 16 and 4-slices Toshiba Asteion 4 Edition. The x-ray generator dose estimation of MDCT scanners performed under details technique parameters (kVp, mAs and exposure time) had been assessed using multi-function detector (Raysafe Unfors), TLD-100™ and nanoDot™ OSLDs. The assessment of weighted CT Dose Index (CTDIw) is measured using 100 mm standard pencil beam ion chamber, TLD-100™ and nanoDot™ OSLDs, in a 160 mm diameter head and 320 mm diameter body cylindrical acrylic Polymethyl-Methacrylate (PMMA) phantom (160 mm length). CTDIw values were specified either in central axis or 10 mm from the 4 outer edge of the phantom. The comparison between two sizes of phantoms made from measurements of the CTDIw in two types of CT scanners. The weighted CTDIs (CTDIw) were calculated and CT x-ray generator performance were observed. The results using three different type of detectors were examined and compared. The deviation accuracy of the tube voltage lied in between ±5 kV or ±5% whichever is greater, whereas the accuracy of exposure time and coefficient of linearity (mAs) lied in between ±10%. The radiation dose (CTDIw) to dose under exceptional CT scanning condition during axial modes were observed to meet the manufacturer guideline (<±20%). The implement CT dosimetry steps ensured the patient safety and can reduce future risk if an estimated dose value is inappropriately above the relevant threshold for any routine CT examination.

Contact author: Ratna Suffhiyanni Omar; ratnasuffhiyanni@gmail.com

Acknowledgement: This work was supported by the Ministry of Higher Education Malaysia and Universiti Teknologi Malaysia through UTM Zamalah Scholarship and Research University Grant Scheme (No. 17H79 and 03G72).

Keywords: MDCT, CTDI, PMMA phantom

ID #14: Scattered Dose Measurement for a Mobile C-Arm Fluoroscopy System: Patient Thickness Factor

Syarul Iman Saufi[1] and Husaini Salleh[2]

[1]Nuclear Medicine Department, Hospital Sultanah Aminah, 80100 Johor Bahru, Malaysia, [2]Medical Physics Group, Malaysia Nuclear Agency, 43000, Kajang, Malaysia

It is well documented that the scattered radiation is the main contributor to the occupational exposure to the radiation worker. This study aimed to investigate the spatial distribution of scattered radiation doses rate induced by exposure to the C-arm machine (Toshiba SXT-1000A) from irradiated water phantom of different thickness. Water phantoms with different size (10cm), (20cm) and (25cm) were used. They were exposed to X-ray radiation from a mobile c-arm fluoroscopy system with automatic brightness control mode function. An ion chamber (1,800 cc) model Radcal 20X6-1800) was used to measure scattered radiation at two different levels namely abdomen (100 cm from the floor) and eye level (160 cm from the floor). The ion chamber was placed at nine different positions (Point A to I) with source-to-detector distance (SDD); (A: 45cm), (B: 45cm), (C: 60cm), (D: 107cm), (E: 70 cm), (F: 50cm), (G: 90cm), (H: 60cm) and (I: 45cm) around the examination table. The scattered radiation profiles surrounding the phantom was determined. Based on the result, the dose rate of scattered radiation of 25 cm thickness recorded the highest reading (25.60 ± 0.01 mR/hr - 478.60 ± 0.00 mR/hr), followed by the 20 cm thickness (12.66 ± 0.01 mR/hr - 260.90 ± 0.01 mR/hr). It was found that 10 cm thickness phantom recorded the lowest reading among three sizes, (2.24 ± 0.02 mR/hr – 58.66± 0.00 mR/hr). It was noted that the scattered radiation increases linearly with the phantom thickness. Therefore, the radiation protection principle and the concept of ALARA and optimization should be strengthened especially during the clinical procedure inside the Operating theatre (OT) room.

Contact author: Presenting Author: syarul_iman@moh.gov.my

Keywords: scattered radiation, dose meter, mobile c-arm, dose rate, phantom thickness

ID #20: Elemental Evaluation of Urban Road Dirt via a Number of Analytical Techniques

Abdullah Alsubaie[1,2]*, L Alsulaiti[3], Eman Daar[1,4], Abdullah N. Al-Dabbous[5], Mariem Chamakh[4], Maisarah Jaafar[6], DA Bradley[1,7]

[1]*Department of Physics, University of Surrey, Guildford GU2 XH, UK*, [2]*Department of Physics, College of Education and Science – Al Khurma, Taif University, Saudi Arabia*, [3]*Department of Mathematics, Statistics and Physics Qatar University, Qatar*, [4]*Department of Physics, The University of Jordan, Amman, Jordan*,[5]*Crises Decision Support Program, Environment and Life Sciences Research Center, Kuwait Institute for Scientific Research, P.O. Box 24885, 13109, Safat, Kuwait*, [6]*School of marine and environmental sciences,Universiti Malaysia Terengganu, 21030 Kuala Nerus,Terengganu,* [7]*Sunway University, Centre for Biomedical Physics, Jalan Universiti, 46150, PJ, Malaysia*

Worldwide, toxicological consequences are arising from vehicular contributions to environmental pollution. Herein, elemental monitoring has been conducted of road dirt via a number of analytical techniques, sampling being made along the busy campus roads of universities/research institutes in Guildford, Riyadh, Kuwait City, Doha and Kuala Lumpur. Using ICP-OES and ICPMS techniques, absolute values have been determined for Ti, Mn, Co, Zr, Mo, Ba, Tl, V, Rd, Cu, Zn, Ni, Cr, Cd, As and Hg, while an SEM/EDX technique has provided weight % values. Results are compared, both qualitatively and quantitatively. Al, Fe, Mg, and Si have been found to be the most prominent elements in road samples, particularly in respect of the Gulf countries and are in agreement with values observed in previous work by the same group, use being made of XRF, SEM/EDX, ICP-MS and ICP-OES. Furthermore, Mg, Ti, V, Cu, Zn, Ni, Cr and Ba have been observed throughout the different climates, albeit at lower concentrations (minimum to maximum concentrations), with particle sizes of the order of 0.5 micron. In addition, elemental presence is seen to be influenced by climatic conditions as well as vehicle engine size. In conclusion, the various techniques offer complementary information on vehicular emission elemental concentrations in urban environments.

Contact author: Abdullah Alsubaie; a.alsubaie@surrey.ac.uk

Keywords: Road-dirt,/SEM EDX, ICP-MS and ICP-OES spectrometry.

ID #31: Accuracy of Standardized Uptake Value Measurements in metastatic lesion for ^{99m}Tc-HMDP bone SPECT/CT

Khairul Nizam Jaafar[1] and Syahir Mansor[1,2]

[1]Nuclear Medicine Unit, Advanced Medical and Dental Institute, Universiti Sains Malaysia, 13200 Kepala Batas, Penang, Malaysia, [2]Oncological and Radiological Science Cluster, Advanced Medical and Dental Institute, SAINS@BERTAM Universiti Sains Malaysia, 13200 Kepala Batas, Penang, Malaysia

Advance development of iterative image reconstruction enables absolute quantification of SPECT/CT studies by incorporating compensation for collimator-detector response, attenuation, and scatter into the reconstruction process. The aim of this study is to assess its quantitative accuracy for potential clinical ^{99m}Tc-HMDP SPECT/CT application in the metastatic bone lesion.

Uniform Jaszczak phantom equipped with six fillable spheres was filled with an activity ratio of 10 to 1 for sphere and background respectively and acquired on a SPECT/CT gamma camera (Discovery 670; GE Healthcare). Subsequently, volume-of-interest (VOI) of each sphere was drawn on SPECT using various methods on CT images. In addition to that, retrospective data of patient who underwent bone scan was acquired. Various VOIs were drawn on the metastatic lesion in the spine, rib while normal spine and lung as a reference for the normal region.

The convergence of activity concentration was dependent on iteration number and application of post filtering. SUV*mean* metric shows an underestimation about 40% from the actual SUV while SUV*max* shows and overestimation about 20% for the largest diameter sphere. The reduction of bias as much as -20% and -1.5% for SUV*0.6max* and SUV*0.75max* respectively. Patient study results were consistent with the phantom validation. Absolute SPECT/CT quantification of bone metastatic lesion studies using ^{99m}Tc-HMDP seems feasible with < 8% deviation (19.7 mm diameter sphere) when using SUV*0.75max* as a metric, and sufficient iteration was used. However, with irregularities shape of metastatic lesions, the quantification evaluation should be further validated.

Contact author: Syahir Mansor; syahir.mansor@usm.my

Acknowledgment: This study was supported by Universiti Sains Malaysia (USM), Short Term Grant 304/CIPPT/6315160.

Keywords: SPECT/CT, SUV, quantitative, ^{99m}Tc-HMDP, phantom

ID #34: Estimation of absorbed dose to lungs and heart in pediatric chest x-ray examination at different tube voltages: Phantom study

Inayatullah Shah Sayed[1], Nurul Hazwani Md Jamal[1], Waliullah Shah Syed[2]

[1]Department of Diagnostic Imaging and Radiotherapy, Kulliyyah of Allied Health Sciences, International Islamic University Malaysia, Jalan Sultan Ahmad Shah, Bandar Indera Mahkota, 25200 Kuantan, Pahang, Malaysia; [2]School of Health Sciences, Universiti Sains Malaysia, Health Campus, 16150 Kuban Kerian, Kota Bharu, Kelantan, Malaysia

Children have a greater risk of developing lifetime cancer and other biological effects from ionizing radiation exposure, than adults. The aim of this study was to measure the absorbed dose received by lungs and heart in pediatric chest x-ray examination by using nanoDot optically stimulated luminescent dosimeter (OSLD). The x-ray system, Siemens Multix Top was used. A pediatric phantom developed by using beeswax and polyurethane foam was exposed at 50, 52 55, 57 and 60 kVp, with fixed tube current (3 mAs), which is normally used in pediatric clinical chest x-ray examinations. The nanodot OSLDs were placed in different parts in the thorax of the phantom according to the position of organs in the chest area, which are lungs and heart. For lungs, absorbed dose measurement nanoDot OSLDs were placed in the apex and base at three different depths. The phantom was exposed three times for each kVp value, and the absorbed doses were measured in mGy. The findings show that the measured absorbed dose to the heart increased with the increase in kVp. Overall, a 22% increase in absorbed dose to heart was recorded. And a 29% increase in lungs absorbed dose with the increase in kVp was recorded. In addition, absorbed dose to the base of left and right lungs was recorded higher up to 9% as compared to the apex of lungs. However, the exit-dose of lungs reduced by 20%. In conclusion, the absorbed dosage increases with exposure, while the absorbed dose decreases with depth. It is necessary for the radiographer to select an appropriate exposure setting based on the physical characteristics of the pediatric patient.

Contact author: Presenting Author; inayatullah@iium.edu.my

Acknowledgement: The authors would like to acknowledge the Department of Diagnostic Imaging and Radiotherapy, Kulliyyah of Allied Health Sciences, International Islamic University Malaysia (IIUM) for providing the facilities and equipment to carry out the study. This research is supported by the International Islamic University Malaysia under the Research Initiative Grant Scheme, RIGS #16-302-0466.

Keywords: absorbed dose, chest X-ray, pediatrics, phantom, OSLD

ID #35: Scattered radiation dose to caregivers' in plain radiography: A case study

Inayatullah Shah Sayed[1], Nurfadhilah Hanani Yusri[1]

[1]*Department of Diagnostic Imaging and Radiotherapy, Kulliyyah of Allied Health Sciences, International Islamic University Malaysia, Jalan Sultan Ahmad Shah, Bandar Indera Mahkota, 25200 Kuantan, Pahang, Malaysia.*

In radiography it is imperative to protect patients and their caregivers from adverse effects of x- radiation when they undergo diagnostic procedures. However, in certain circumstances some radiation practitioners ignore radiation protection measures that should be practiced during x-ray examinations and allow the next-in-line patient and caregiver to wait behind x-ray lead barrier inside the radiography room till the earlier patient's examination is complete. The purpose of this case study was to measure scattered radiation dose at six different heights in the x-ray room at specific positions that might be received by patient's caregiver. Siemens Multix Top x-ray system was used. Anthropomorphic phantom Kyoto Kagaku Phantom PBU-50 (torso) was scanned by positioning supine on examination table for anteroposterior (AP) lumbar projection. Optically stimulated luminescent (OSL) dosimeters were fixed on a wooden stick at 120, 130, 140, 150, 160 and 170 cm heights with respect to the floor. The stick was fixed in such a way to stand vertically behind the x-ray lead barrier at 2.5 meters distance from the x-ray tube. The phantom was exposed by selecting tube voltages of 68, 79 and 90 kVp at a constant tube current, 32 mAs fixing a 100 cm source to image distance (SID). Results showed that scatter radiation doses measured at different heights were different for each exposure. The highest scattered radiation dose measured was 0.0064 mGy and 0.0042 mGy at 130 cm height for 79 kVp and 90 kVp exposures, respectively. It is concluded that the measured scattered radiation doses were within the acceptable dose limits as recommended in ICRP Publication 105 for patient comforter. Nonetheless, the malpractice should not be ignored because it exposes the individual to unnecessary radiation.

Contact author: Presenting Author; inayatullah@iium.edu.my

Acknowledgement: The authors would like to acknowledge the Department of Diagnostic Imaging and Radiotherapy, Kulliyyah of Allied Health Sciences, International Islamic University Malaysia (IIUM) for providing the facilities and equipment to carry out the study. This research is supported by the International Islamic University Malaysia under the Research Initiative Grant Scheme, RIGS #16-302-0466.

Keywords: radiation protection, scattered radiation, plain radiography, OSLD

ID #37: Radiation dose and Size Specific Dose Estimate from CT Pulmonary Angiography examinations

H H Harun[1], M K A Karim[1], N A Muhammad[1], A Sabarudin[2], S C Muniandy[3]

[1]Department of Physics, Faculty of Science, Universiti Putra Malaysia 43400 Serdang, Selangor, Malaysia; [2]Department of Diagnostic & Applied Health Sciences, Faculty of Health Sciences, Universiti Kebangsaan Malaysia, Jalan Raja Muda Abdul Aziz,50300 Kuala Lumpur, Malaysia; [3]Department of Radiology, Hospital Kuala Lumpur, Jalan Pahang, 50586 Kuala Lumpur, Malaysia

The number of Computed Tomography (CT) scan examinations has increased gradually owing to its advantages in providing high contrast diagnostic images. Despite continuous demand of the examination, the public and radiology personnel towards CT radiation dose is remains a concern. The purpose of this study is to evaluate radiation exposure for adult patients undergoing CT Pulmonary Angiography (CTPA) examinations based on the size-specific dose estimate (SSDE) and volume CT Dose Index (CTDIvol). We perform a retrospective study comprised of 30 patients (with age in year old range from 18 – 50 y/o) undergoing CTPA examinations. Scanning parameter data and radiation dose measures included diameter of antero-posterior and lateral, tube potential, tube current and CTDIvol. SSDE value were obtained from two type of calculations technique, AAPM report 204 recommendation and CT EXPO (Ver 2.3.1, Germany) software. The ratio of SSDE to CTDIvol was 1.63 and 1.41 for ≤25 cm effective diameter (n= 12) and >25 cm effective diameter (n = 18), respectively. The mean SSDE value were 13.49±6.09 mGy ($p<0.001$) and 14.40±6.38 mGy ($p<0.001$) estimated from AAPM recommendation and CT EXPO calculation, respectively. Both values were higher than CTDIvol from consoles indicate the patient's f-size was larger than 1.0. In conclusion, we established different approach of determining radiation dose based on patient size and composition in order to further standardization of scanning protocols and staff training.

Contact author: H H Harun; hanifhaspi@gmail.com

Acknowledgement: The authors wish to acknowledge the support from Geran Putra IPM of Universiti Putra Malaysia with project no. GP/IPM/9619800 and Radiology staffs from Hosiptal Kuala Lumpur

Keywords: Computed Tomography, SSDE, CT Pulmonary Angiography.

ID #38: Cumulative Effective Dose in Adult Patients Population Undergoing Repeated or Multiple Head CT Scanning

Mohd Amirul Azrie Mohd Roslee[1], Ibrahim Lutfi Shuaib[1], Ahmad Fakharuddin Mohd Napi[2], Mohd Amir Syahmi Mat Razali[1], Noor Diyana Osman[1]

[1]*Advanced Medical and Dental Institute, Universiti Sains Malaysia, Kepala Batas, Penang, 13200, Malaysia;*
[2]*Department of Radiology, Hospital Universiti Sains Malaysia, Kubang Kerian, Kelantan, 11800, Malaysia*

The computed tomography (CT) scan is the most frequently used in diagnostic imaging. The current concern is related low radiation dose to patients and the potential radiation-related health effects due to multiple CT exposures. This study was aimed to evaluate cumulative organ dose received from multiple exposures in adult patients underwent CT head examination. The retrospective dose survey was performed at AMDI,USM and HUSM. A total of 202 adult patients had multiple exposures selected. The organ doses were estimated using CT ImPACT program. From the survey, most of the patients received 3 times head CT examinations. The highest organ dose was observed at lens with the value of 7.125 mSv for 13 exposures followed bythyroid with values of 7.48 mSv. Based on ICRP recommendation, the highest mean value of 7.48 mSv received by thyroid was considered atlow risk and within the range of 0.1-8 % below 100 mSv. Furthermore, organ dose received by lens was at low risk of cataract. However the increasing of multiple exposure will lead to dose contribution (p-value = 0.01). Moreover, the absorbed dose of the lens received after 4 exposures exceeded the rangeof 2 Gy of cataract risk with the M =242.05, p= 0.01.Besides, the mean cumulative effective dose by simple and CT ImPACT calculation were 32.1 mSv and 43.8 mSv (p-value = 0.01). The selection of effective dose calculation is important for an accurate outcome and dose received after multiple exposureson the same patients should be limited.

Contact author: Mohd Amirul Azrie Mohd Roslee; amirul.azrie@usm.my

Acknowledgement: The authors would like to thank all staff at Imaging Unit of AMDI and HUSM Kubang Kerian for their help and support throughout this work. We would also like to express our deep gratitude to Medical Dosimetry Group, Centre for Radiation, Chemical and Environmental Hazards (CRCE), Public Health England (PHE) for their data sharing related to this work.

Keywords: Cumulative organ dose, Effective dose, Multiple CT exposure

ID #42: Dose Optimisation in Paediatric CT Examination: Assessment on Current Scanning Protocols Associated with Radiation Dose Received

Muhammad Kabir Abdulkadir[1,2], Nur Atikah Yusra Mat Rahim[3], Nur Syazwani Mazlan[3], Norfataha Mohd Daud[4], Noor Diyana Osman[1]

[1]Advanced Medical and Dental Institute, Universiti Sains Malaysia, Kepala Batas, Penang, 13200, Malaysia; [2]Department of Medical Radiography, Faculty of Basic Medical Sciences, University of Ilorin, 240213, Nigeria; [3]School of Health Sciences, Health Campus, Universiti Sains Malaysia, Kubang Kerian, Kelantan, 11800, Malaysia; [4]Department of Radiology, Hospital Universiti Sains Malaysia, Kubang Kerian, Kelantan, 11800, Malaysia

Request for paediatric CT imaging has been increasing recently, to assess the associated potential risk and possibly identify need to modify the current practice, assessment of current paediatric protocols is of crucial importance. The aim of this study was to optimize the current practice through investigation of the radiation dose and existing routine acquisition protocols of paediatric CT imaging for head and abdomen examination at HUSM, Kelantan, Malaysia. A total of 150 CT paediatric (0-12 years) examinations (85 brains CT and 65 abdominal CT) were retrospectively collected from PACS and analyzed. Dose estimates in volumetric dose index (CTDIvol) and dose length product (DLP) and combination of exposure parameters kV, mAs, pitch, scan length and acquisition time currently in use for paediatric imaging were evaluated. Third quartile of our dose values were then compared with international standards and other countries. Estimated dose values in CTDIvol (mGy) and DLP (mGy.cm) for head and abdominal CT scans with respect to the age groups are 0-3 years (32/494 and 7/194), 4-6 years (63/1087 and 9/319), 7-9 years (59/1258 and 9.5/397), 10-12years (118/2215 and 13/498) respectively. Tube voltage selection was ranged from 100-120 kV for all groups except head scans in group 4 that used a constant 120 kV. Applied mAs vary and increases from group 1- 4 and ranges from 100-410 mAs for head scans and 35-100 mAs for abdominal scans. In this study, dose received from paediatric head CT scans were above the recommended levels. This is mainly due to selected acquisition parameters and hence, need for optimization of current protocols.

Contact author: Muhammad Kabir Abdulkadir; Kabirkad@yahoo.com

Keywords: Computed Tomography, Paediatric, Dose Optimization

ID #44: Scatter cloud radiation in fluoroscopy-guided interventional (FGI) room

Asmah Bohari[1], Suhairul Hashim[1,2] and Siti Norsyafiqah Mohd Mustafa[3]

[1]Department of Physics, Faculty of Science, Universiti Teknologi Malaysia, 81310 UTM Skudai, Johor, Malaysia; [2]Centre for Sustainable Nanomaterials (CSNano), Ibnu Sina Institute for Scientific and Industrial Research (ISI-SIR), Universiti Teknologi Malaysia, 81310 UTM Skudai, Johor, Malaysia; [3]Department of Radiology, Institut Kanser Negara, 62250 Putrajaya, Wilayah Persekutuan Putrajaya, Malaysia

Fluoroscopic imaging generates radiation fields that are unevenly scattered throughout the fluoroscopy-guided interventional (FGI) room. We wanted to quantify the radiation dose scattered at various locations during FGI procedures for clinical use. Digital subtraction imaging (Philips Allura Xper FD20/20, Philips Healthcare) of the abdomen was a performed-on Sawbones torso in standard anteroposterior (AP), left anterior oblique 45 (LAO45), left anterior oblique 90 (LAO90) and right anterior oblique 45 (RAO45) projection. Radiation exposure was monitored using optically stimulated luminescence dosimeter (OSLD). OSLD were placed on long pipe with height 100 cm from the floor. The OSLDs were readout using microStar reader system (Landauer, Inc.). With AP imaging, the radiation fields have symmetric bell shape, with maximal exposure perpendicular to patient table at the level of the gantry. Peak level at 75 cm from the source emitter were 5 times higher than the inverse square law. Maximal radiation exposure was measured in position 50 cm away and perpendicular to the table (13.32 mSv/h). When the gantry was rotated to LAO45 and LAO90, the radiation fields increased radiation doses to 28.65 and 22.99 mSv/h, respectively. Nevertheless, at the RAO45 was decreasing to 17.4 mSv/h. Minimal exposure is experienced along the axis of the table, decreasing with distance from the source (<0.33 mSv/h). Reproducible and observable scatter radiation is created during FGI procedure. Dose of radiation vary widely around the perimeter of the patient table and change according to imaging angles. Knowledge of the exposure levels may help in justifying the risks to staff.

Contact author: asmahbohari@gmail.com

Acknowledgement: This work was supported by the Malaysian Ministry of Education and Universiti Teknologi Malaysia through the Research University Grant Scheme (No. 17H79 and 03G72). The study protocol was approved by the National Medical Research Register (NMRR-17-2092-34972) and Malaysian Ethical Research Committee (MREC(5)KKM/NIHSEC/P17-1524). Confidentiality of all personal details of the subjects was retained.

Keywords: scatter cloud, OSLD, interventional

ID #46: Small angle neutron scattering studies of dipalmitoylphosphatidylcholine-hyaluronic acid vesicle structural properties

Irman Abdul Rahman[1,2], Hur Munawar Kabir Mohd[1], Faizal Mohamed[1,2], Kenton P. Arkill[3], Shahidan Radiman[1,2], David A. Bradley[4,5]

[1]Nuclear Technology Research Centre, Faculty of Science and Technology, Universiti Kebangsaan Malaysia, 43600 Bangi, Selangor, Malaysia; [2]Centre for Frontier Sciences, Faculty of Science and Technology, Universiti Kebangsaan Malaysia, 43600 Bangi, Selangor, Malaysia; [3]School of Medicine, University of Nottingham, Nottingham, United Kingdom. [4]Sunway University, School of Healthcare and Health Sciences, Centre for Biomedical Physics, No. 5, Jalan Universiti, Bandar Sunway, 47500 Petaling Jaya, Selangor, Malaysia, [5]Department of Physics, Faculty of Engineering and Physical Sciences, University of Surrey, Guildford, GU2 7XH, UK

We investigated the structural property changes that dipalmitoylphosphatidylcholine (DPPC) vesicles underwent after addition of hyaluronic acid (HA) using small angle neutron scattering (SANS). The functionality and stability of DPPC-HA vesicles especially as synovial fluid bio-lubrication component correlates with their structural properties. Vesicles were studied through detailed SANS data analysis on the colloidal fractal aggregation process using dynamic light scattering (DLS) and SANS. SANS results demonstrated that both DPPC and DPPC-HA vesicles showed mass fractality properties that produces a slope between -1 and -3 in a log-log Q-*I*(Q) plot. The slope and knee features of the scattering curves of both vesicles indicate the vesicle structure and shape. Additionally, the DLS (size and polydispersity) results were also used to explain the colloidal behaviour of the vesicles systems and their aggregation process.

Contact author: Irman Abdul Rahman; irman@ukm.edu.my

Acknowledgement: This work was supported in part by the Royal Society and the Academy of Sciences Malaysia through Newton-Ungku Omar Fund (ST-2018-022) and UKM Research University Grant (GUP-2018-060). We also thank the High-flux Advanced Neutron Application Reactor (HANARO) in Korea Atomic Energy Research Institute (KAERI) for allowing us to use SANS instrument.

Keywords: Lipid vesicle, hyaluronic acid, mass fractal, small angle neutron scattering

ID #51: Mass attenuation coefficients of *Rhizophora* spp. particleboards incorporated with metal elements as shielding materials at 16.59-25.26 keV photons

Siti Nor Azizah Abdullah[1], Mohd Fahmi Mohd Yusof[2], Norlaili Ahmad Kabir[1], Rokiah Hashim[3], Abd Aziz Tajuddin[4]

[1]School of Physics, Universiti Sains Malaysia, 11800 Penang, Malaysia; [2]School of Health Sciences, Universiti Sains Malaysia, 16150 Kota Bharu, Kelantan, Malaysia; [3]School of Industrial Technology, Universiti Sains Malaysia, 11800 Penang, Malaysia; [4]Registrar, Albukhary International University

The study focused on the fabrication and attenuation evaluation of *Rhizophora* spp. particleboards incorporated with metal elements as potential shielding materials for low energy photons. The *Rhizophora* spp. particleboards were fabricated at density of 1.0 g/cm^3 and incorporated with $BaSO_4$ and Bi_2O_3 at 5, 10 and 15% percentage levels. The mass attenuation coefficients of the particleboards were measured by using the x-ray fluorescent (XRF) photons between 16.59 and 25.26 keV energies. The results showed that the mass attenuation coefficients of the particleboards increased when higher percentage levels of metal elements were used. The particleboards incorporated with Bi_2O_3 showed significantly higher mass attenuation coefficients that the particleboards incorporated with $BaSO_4$. A comparison to the XCOM values of the metal elements showed that the particleboards incorporated with the highest percentage of Bi_2O_3 showed the nearest mass attenuation coefficients to the $BaSO_4$. The overall results indicated the possibilities of the fabrication of shielding materials from *Rhizophora* spp. particleboards for low energy photons.

Contact author: Mohd Fahmi Mohd Yusof; mfahmi@usm.my

Acknowledgement: The authors would like to thank the financial aid of RUI Grant scheme no. 1001/PFIZIK/811345 by Universiti Sains Malaysia.

Keywords: *Rhizophora* spp., shielding materials, mass attenuation coefficients

ID #54: Adaptive region growing image segmentation algorithms for Breast MRI

Joe Arun Raja[1], Nelson Kennedy Babu[2]

[1]Subbalakshmi Lakshmipathy College Science, Madurai, Tamilnadu, 625022, India; [2]SMK Fomra Institute of Technology, Chennai, Tamilnadu, 603103, India

Early detection and characterization of breast lesion are important for a better and effective treatment of breast cancer. In this paper, four different adaptive region growing image segmentation algorithms are compared. In fact, seed selection was a vital step in the success of region growing methods, so, better schemes for seed selection methods are proposed, namely, joint probabilistic seed selection (JPSS) and Generalised simulated annealing (GSA) based seed selection. The proposed region growing methods namely Fuzzy Region Growing (FRG) and Neutrosophic Region Growing (NRG) are integrated as JPSS-FRG and GSA-NRG frameworks. Another two methods are Scale Invariant Region growing (SiRG) and Fuzzy Neutrosophic Confidence Region growing (FNCRG). The results showed that FNCRG algorithm increases breast cancer detection rate on MRI breast images with the maximum of 93% is achieved. SiRG algorithm improves the true positive rate by 13% compared to existing methods. Further, GSA-NRG makes better segmentation accuracy by 9% and true positive rate by 12%. Also, JPSS-FRG algorithm enhances segmentation accuracy by 24% and improving the true positive rate by 24% compared to Region Growing-Cellular Neural Network (RG-CNN) and Seeded Region Growing-Particle swarm optimisation (SRG-PSO) methods respectively.

Contact author: Joe Arun Raja; joearunraja@gmail.com

Acknowledgement: -

Keywords: Breast MRI, Fuzzy logic, Neutrosophic logic, Breast Cancer Image Biomarker, Region growing algorithm

ID #57: Effect of Gamma Irradiation on Magnetic Gadolinium Oxide Nanoparticles Coated with Chitosan (Gd-CsNPs) as Contrast Agent in Magnetic Resonance Imaging

Faizal Mohamed[1], Irman Abdul Rahman[1], Mohd Idzat Idris [1], David Andrew Bradley[2,3], Muhammad Zul Azri Muhammad Jamil[1], Nur Ratasha Alia Md. Rosli[1], Marlida Md Nor[1], Siti Norsyafiqah Mohd Mustafa[4]

[1]School of Applied Physics, Faculty Science & Technology, Universiti Kebangsaan Malaysia, Bangi, Selangor, 43600, Malaysia, *[2]Department of Physics, University of Surrey, Guildford, Surrey GU2 7XH, United Kingdom*, *[3]Centre for Biomedical Physics, School of Healthcare and Medical Sciences, Sunway University, Petaling Jaya, Selangor, 47500, Malaysia, [4]Radiology Department, National Cancer Institute, Kementerian Kesihatan Malaysia, Putrajaya, 62250, Malaysia*

Gadolinium based activation-guided irradiation by X-ray (AGuIX) nanoparticle is a promising theranostic agent candidate in the biomedical field. However in reducing the risk of nephrogenic systemic fibrosis (NSF) currently faced by renal failure patients, the size of the nanoparticle is of importance in being small to be rapidly eliminated via the renal route. This study elucidates a gamma irradiation-reduction approach in synthesizing small gadolinium nanoparticles specifically chitosan coated gadolinium oxide nanoparticles (Gd-CsNPs). Chitosan was used as a natural stabilizer and coating agent whereas gadolinium (III) chloride hexahydrate (GdCl3.6H2O) was used as a precursor. The properties of the synthesized Gd-CsNPs were studied in term of molecular conformation, surface plasmon resonance and particle distribution via ultraviolet-visible spectroscopy (UV-Vis), transmission electron microscopy (TEM) and Fourier transform infrared spectroscopy (FTIR) characterization. Formation of two new UV-Vis peaks at 260 nm and 290 nm depicts the chemical changes of chitosan post gamma irradiation with visible surface plasmon resonance band correlating the reduction of particle size. Further analysis via TEM demonstrates that synthesized Gd-CsNPs had an average diameter size in the range of 30 - 45 nm post gamma irradiation, a reduction of size in comparison with control Gd-CsNPs of 120 nm particle size. Enhancement of T1 image obtained via magnetic resonance imaging (MRI) testing proved the capability of synthesized Gd-CsNPs as a contrast agent. Coherently, gamma irradiation-reduction method may be used in controlling the size of nanoparticle and potentially be applied in all major fields related to gadolinium nanoparticle coated with chitosan like biopolymer.

Contact author: Faizal Mohamed; faizalm@ukm.edu.my

Acknowledgement: The work was financially supported by University Research Grant (GUP-2016-015) and Fundamental Research Grant Scheme (FRGS/1/2017/STG02/UKM/02/8). The author expresses gratitude to the staffs of the National Cancer Institute and Universiti Kebangsaan Malaysia Centre of Research & Instrumentation Management (CRIM) for their assistance in the testing of sample via MRI and also the characterization of samples using UV-vis, FTIR and TEM.

Keywords: gadolinium nanoparticle, gamma irradiation-reduction method, contrast agent

ID #62: Occupational Exposure of the operator Eye Lens in digital coronary angiography and interventions

Esam Mattar[1], Amna J. Al-Jabri[2], K. Alsafi[3], A. Sulieman[4], I.I. Suliman[5,6,*]

[1]Department of Radiological Sciences, College of Applied Medical Sciences, King Saud University, P.O Box 10219 Riyadh 11433, Saudi Arabia, *[2]Department of Radiology and Molecular Imaging, Medical Physics Section, College of Medicine & Health Sciences, Sultan Qaboos University, P.O. Box 35, Al-Khod,123, Oman*, *[3]Department of Radiology, Medical Physics Unit; King Abdul Aziz University; P.O. Box 80215, Jeddah 21589, Kingdom of Saudi Arabia*, *[4]Prince Sattam bin Abdulaziz University, College of Applied Medical Sciences, Radiology and Medical Imaging Department, Alkharj, Kingdom of Saudi Arabia*, *[5]Al Imam Mohammad Ibn Saud Islamic University (IMSIU), College of Science, Physics Department, Committee on Radiation and Environmental Pollution Protection,, Riyadh 11642, Saudi Arabia*, *[6]Sudan Atomic Energy Commission, Radiation Safety Institute, P.O. Box 3001, Khartoum, Sudan*

Patient and staffs in interventional cardiology receive high doses that often exceed the threshold for tissue reactions. Radiation dose reduction in these procedures was therefore become a universal goal. The aim of this study is determination of eye lens dose to operator during cardiac angiography (CA) and percutaneous coronary interventions (PI). Air kerma-area product (P_{KA}) was extracted from DICOM header concerning 250 patients who underwent CA and PCI procedures. Procedures were performed using biplane digital fluoroscopy system with flat-panel detectors. kerma-area product to eye lens dose conversion coefficients derived from literature were used to retrospectively estimate operator eye lens doses to 8 cardiologist who performed on average 20-40 IC procedures each during three month period. Based on literature review, P_{KA} to eye lens dose conversion coefficients ranged from 0.8 to 2.2 $\mu Sv.Gy^{-1}cm^{-2}$ (Median: 1 $\mu Sv.Gy^{-1}cm^{-2}$). Only two cardiologists were observed using eye lens glasses and thyroid gland radiation protection tools. The Occupational exposure dose reduction factors were applied to obtain corrected eye lens dose levels. The estimated operator eye lens doses ranged from: 45.3 to 73.0 μSv per procedures in CA and from: 92.9 to 207.8 μSv per procedures in PCI. These doses are comparable to those presented in the literature and are very close estimated annual effective dose limit. These results provide a starting data point for institutional evaluation of operator eye lens doses in interventional cardiology for optimization radiation protection of the staff in interventional cardiology.

Contact author: Ibrahim I. Suliman; i.i.suliman@gmail.com;

Acknowledgement: Occupational exposure, operator eye lens dose, interventional cardiology, radiation protection.

ID #70: A Study on the Effect of Various Objects' Angulation from the Central Location on Image Displacement due to X-ray Beam Divergence (Image Technical Evaluation)

Zafri Azran Abdul Majid[1], Siti Aisyah Munirah binti Bohang[1], Mohd Syahriman Mohd Azmi[2]

[1]Department of Diagnostic Imaging and Radiotherapy, Kulliyyah of Allied Health Sciences, International Islamic University Malaysia, Jln. Sultan Ahmad Shah Bandar Indera Mahkota 25200 Kuantan, Pahang, Malaysia, [2]Department of Physics, Faculty of Science and Mathematics, Universiti Pendidikan Sultan Idris 35900 Tanjong Malim, Perak, Malaysia.

Introduction: X-ray machine tube produced x-ray with beam divergence property. Manipulation of object within the region of x-ray beam divergence caused image displacement effect on radiograph. Pauzi et al. (2014) proved the correlation between x-ray beam divergence and image displacement effect by using multi-parameter double holes contrast-detail phantom (MDHCD). However, there were limited research studies exhibited effects of various target objects' angulations from central location toward image displacement effect. An image technical evaluation will be used in this study by attempted to demonstrate effects of various target objects' angulations from central location on image displacement due to x-rays beam divergence.
Method: This experimental study was conducted in Radiography Lab., IIUM by using angulation distance marker phantom (ADMP). ADMP was used to confirm image displacement effect and its associated factors such as objects' angulation from central location (CL), object to image receptor distance (OID) and distance of markers from focal point. The study was conducted by exposing phantom with x-ray and associated factors involved were manipulated. Image was analyzed by using ImageJ software to measure distance and angular image displacement. Those measurements were also theoretically calculated by using mathematical equations and it was compared with actual measurements to determine accuracy of the result.
Result and discussion: Distance of image displacement (DID) decreased (2.4, 2.1, 1.9) mm with increasing objects' angulation from CL (30º, 45º, 60º) respectively. However, increases in objects' angulation from CL led to an increment in the value of angular image displacement (AID) which was 1.79º, 3.16º, 5.40º respectively. There is no significant different in actual and theoretical values of image displacement effect produced. Besides, increasing angulation of object from CL reduced length of markers depicted on radiograph which were 22.6 mm, 18.4 mm and 13.0 mm respectively. OID and distance of markers from focal point had direct relationship with both DID and AID.
Conclusion: In conclusion, manipulation of various objects' angulation from CL within boundary x-ray beam divergence resulted in image displacement effects. Increased in objects' angulation from CL caused more deviation of marker from control and created larger AID. Recorded length of markers also reduced. ADMP was useful as a quality control (QC) phantom to evaluate image displacement effect and it can be commercialized since its materials were widely available in market.

Contact author: amzafri@iium.edu.my

Keywords: X-ray beam divergence, Distance of image displacement (DID), Angular image displacement (AID), Objects' angulation from central location (CL)

Clinical Oncology

ID #23: Peritoneal-pleural Leaks Demonstrated by Peritoneal Scintigraphy

Khadijah Abdul Hamid[1] and Mohammad Fitri Khalil[1]

[1]*Oncological and Radiological Science Cluster, Advance Medical and Dental Institute, Universiti Sains Malaysia, 13200 Kepala Batas, Penang, Malaysia*

Introduction

Continuous ambulatory peritoneal dialysis (CAPD) is widely used for the long term management of end stage renal failure since the year 1976 (1). It is mainly used for patients who are unable or unwilling to undergo haemodialysis or renal transplant, patients with cardiovascular disease (mainly heart failure), old patient, those who are at risk of adverse effect of systemic heparin, severe hypertension and those who have exhausted their vascular access. The goals of peritoneal dialysis are removing toxic substances and metabolic wastes, reverse the symptom of uraemia, re-establish normal fluid and electrolyte balance and maintaining a positive nitrogen balance. Although it offers several advantages over haemodialysis, there have been several recognized complications. As it is mainly a long term form of usage, it requires intact anatomical integrity of the peritoneal cavity (2). As intraabdominal pressure increases due to the instillation of intraperitoneal fluid, it predisposes the patient to leaks and herniation through defects in the abdominal wall (3). Complication related to usage of peritoneal dialysis such as pleural effusion (due to peritoneal-pleural communication), scrotal swelling (peritoneal-scrotal communication), hernia incarceration and recurrent peritonitis, which all leads to temporary switching to haemodialysis. Investigation that are usually performed such as peritoneal scintigraphy, computerized tomography (CT scan) and peritoneography with iodinated contrast.

Case report

Twenty-three-year-old gentleman with known history of hypertension and end stage renal failure for the past four years was on haemodialysis 3 times a week using arteriovenous fistula. Unfortunately, it was infected and non-functioning for the past 3 months and he used perm catheter for haemodialysis as a temporary measure. Trial of re-inventing the arteriovenous fistula failed after 4 attempts. Due to exhausted vascular access, he was started on continuous ambulatory peritoneal dialysis. He was trained for the continuous ambulatory peritoneal dialysis (CAPD) and discharged well.

However, he developed gradual onset of shortness of breath associated with cough and fever. Chest x-ray was done and revealed massive right pleural effusion (Figure 1). He was admitted and treated with antibiotics. CAPD was withheld and he was switched to haemodialysis using a temporary internal jugular vein catheter. Pleural tapping was done and noted the glucose level of 18.3 mmol/L which is almost similar to peritoneal fluid while his serum blood glucose was only 5.0 mmol/L.

A repeat chest x-ray was done a few days later showed resolution of right pleural effusion (Figure 2). He was referred to nuclear medicine team to rule out peritoneal-pleural leaks of the peritoneal fluids.

119 MBq of Tc-99m nanocolloid mixed with 2.0L of dialysate fluid was slowly infused into the peritoneal cavity through Tenckhoff catheter (Figure 3). Dynamic imaging of abdomen and lower part of thorax was acquired for 30 minutes. Static images of anterior, posterior and lateral of abdomen and thorax was acquired after 30 minutes and delayed 2 hours later.

The first 30 minutes images showed accumulation of tracer within the peritoneal cavity (Figure 4). Static images at 30 minutes showed faint uptake of tracer in the right hemithorax (Figure 5). Images at 2 hours showed more prominent uptake of tracer at right hemithorax (Figure 6). Otherwise there was no abnormal tracer accumulation in the left thoracic cavity or elsewhere. These findings were suggestive of peritoneal fluid leakage into the right thoracic cavity.

Continuous ambulatory peritoneal dialysis for this patient is further withhold till correction of the leakage done. Meanwhile he will continue haemodialysis.

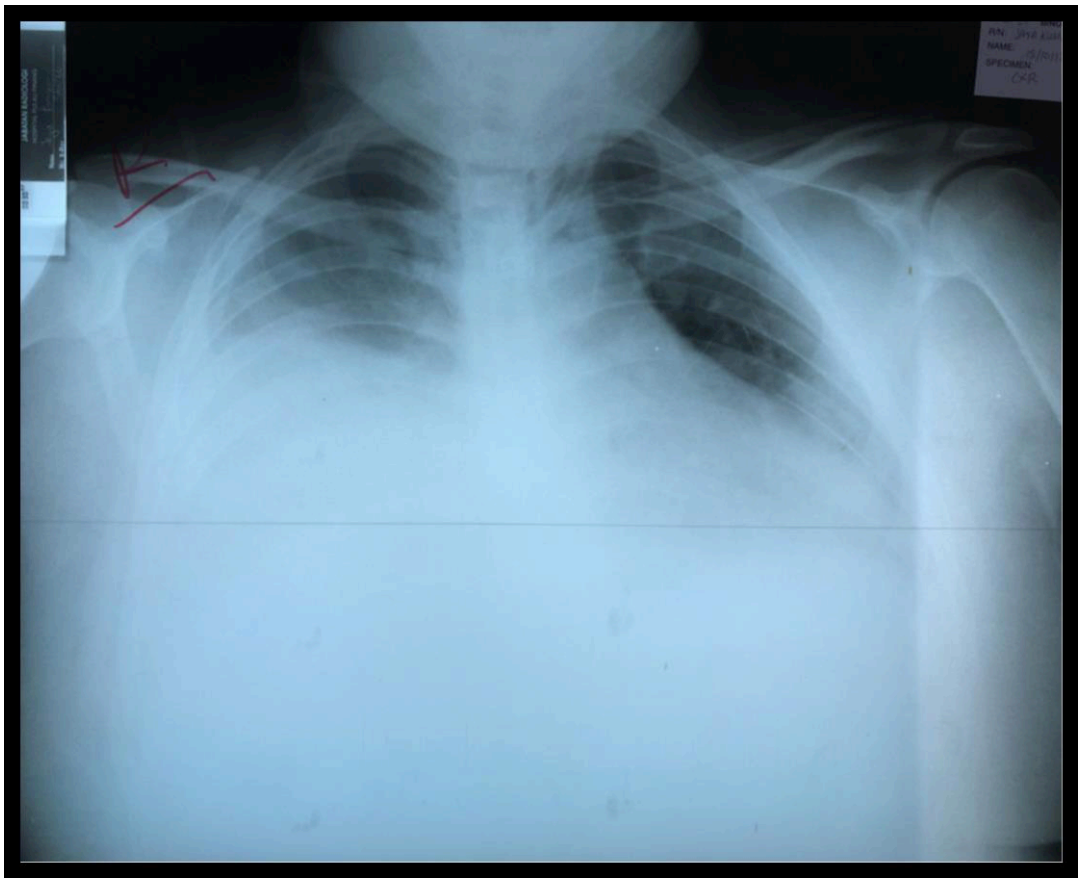

Figure 1. Chest X-ray showed massive right pleural effusion.

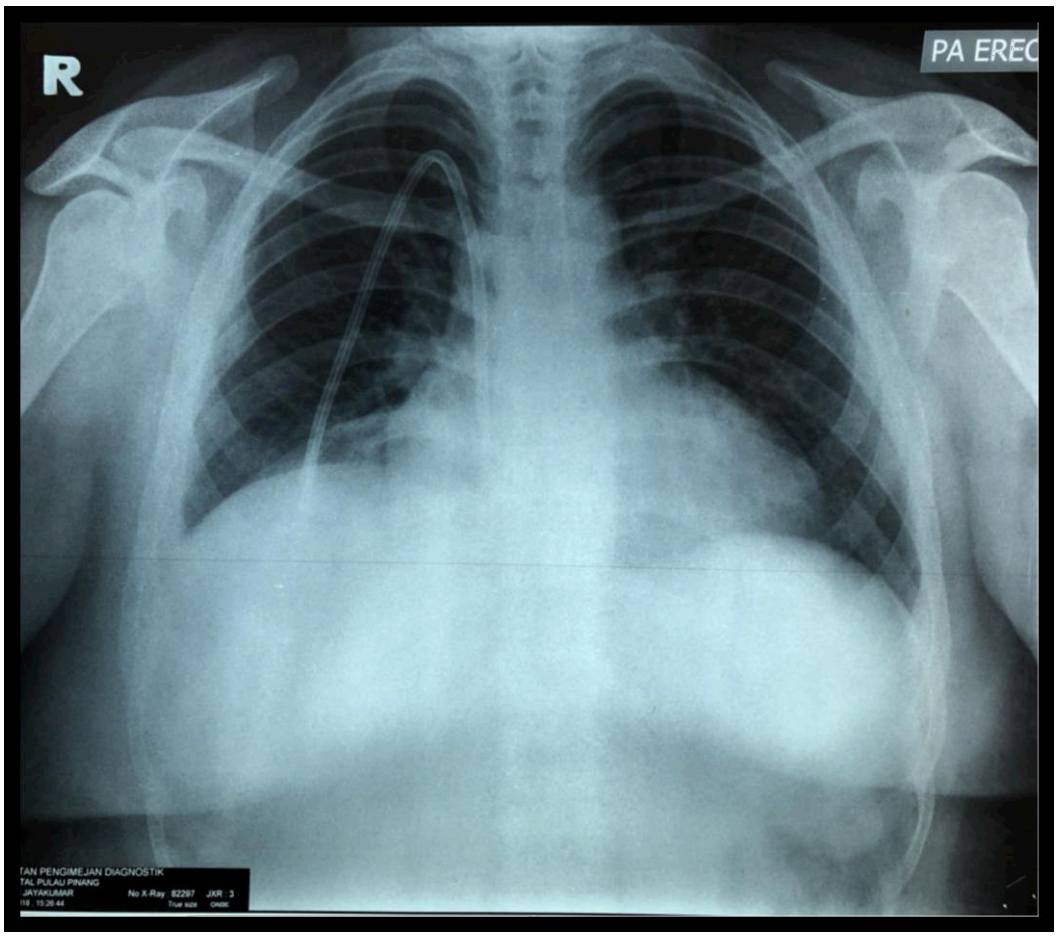

Figure 2. Chest X-ray showed resolution of right pleural effusion.

Figure 3. Tenckhoff catheter in situ.

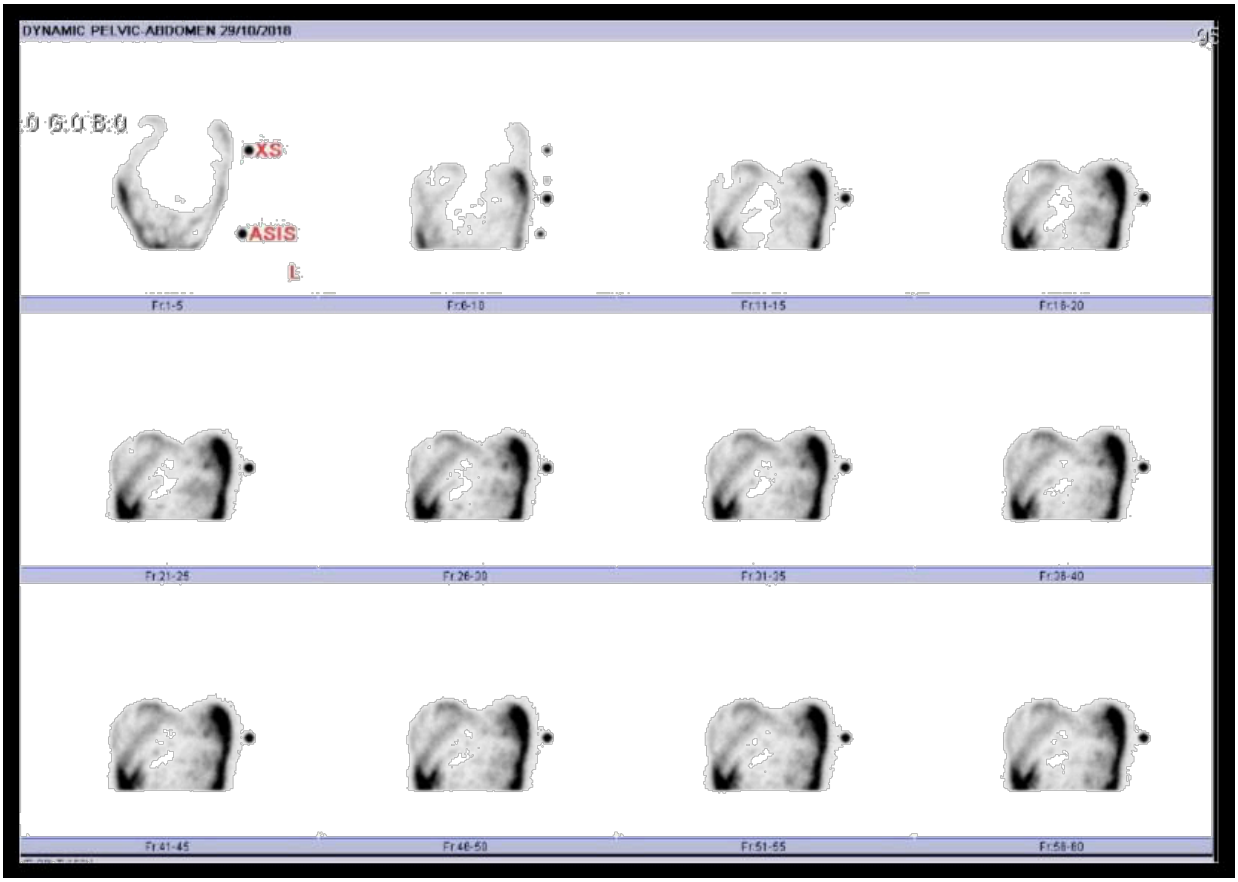

Figure 4. There is accumulation of tracer within the peritoneal cavity during the first 30 minutes of study.

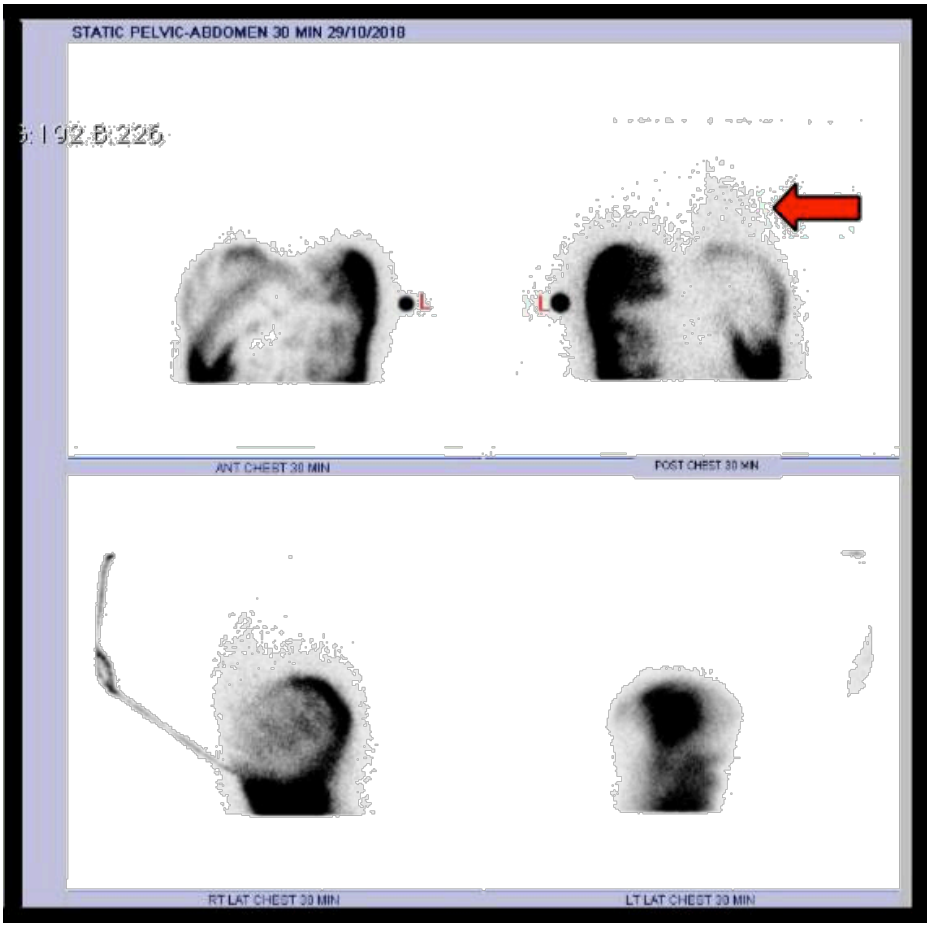

Figure 5. Static imaging - There is faint uptake of tracer in the right hemithorax at 30 minutes (red arrow). It is more prominent in the posterior view.

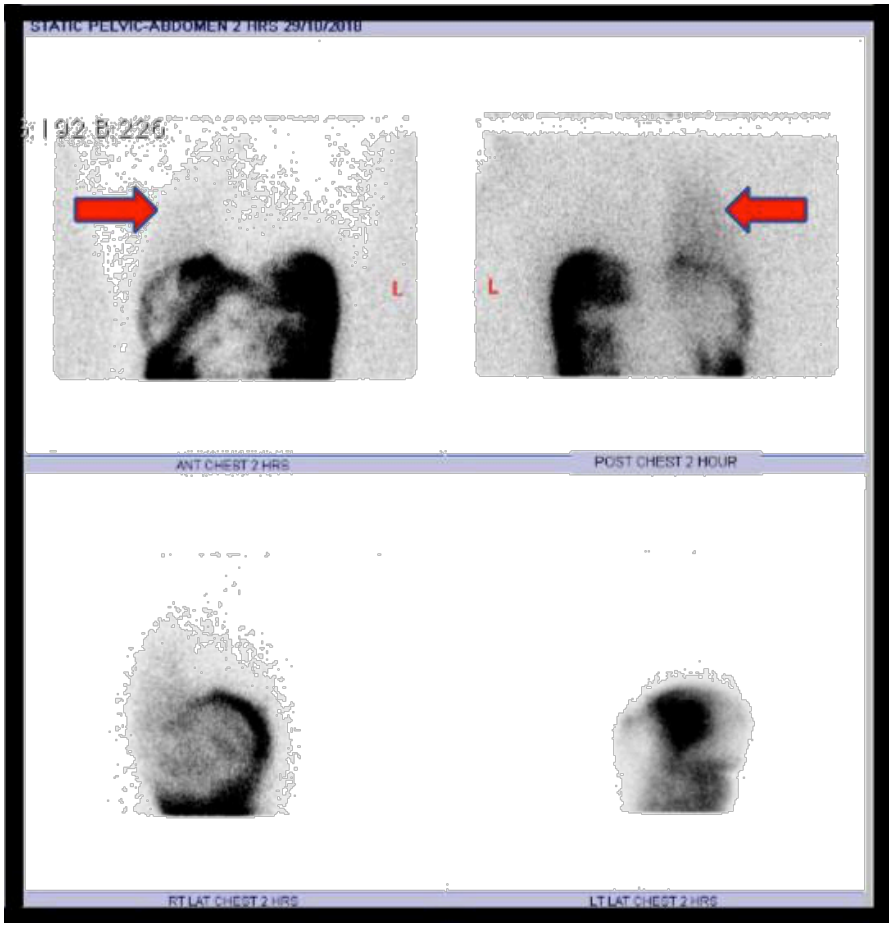

Figure 6. Static imaging - There is more prominent uptake of tracer in the right hemithorax at 2 hours (red arrows).

Discussion

One of the primary complicating factors affecting the long term use of CAPD is loss of the anatomic integrity of the peritoneal cavity (4). Although some of the complication can be detected clinically, it is often necessary to confirm using diagnostic imaging.

Pleural effusion or hydrothorax is uncommon, but it is a well-recognized complication of peritoneal dialysis. Typically patient may develop pleuritic chest pain and shortness of breath. It is caused by migration of fluid into the pleural space via pleuroperitoneal fistula. The reported incidence of pleural effusion in CAPD patient is about 1.6% (5). There is a predominance of right sided pleural effusion, as the defect are usually right sided and congenital (6). Most of the cases happened within the first 30 days of starting the peritoneal dialysis and about 25% of them are asymptomatic (7).

The diagnosis of hydrothorax requires a combination of biochemical and imaging modalities. Pleural fluid biochemistry analysis will usually reveal a transudate with a high glucose concentration. The pleural fluid glucose is affected by the dialysate composition,

and generally accepted that a glucose level of more than 16.5 mmol/L or greater than the serum glucose level is consistent with hydrothorax (8).

Imaging modalities such as computerized tomography scan (CT scan) and MRI are less frequently used compared to peritoneal scintigraphy. Peritoneal scintigraphy has a sensitivity of approximately 50% (8). Radiotracer that are usually used includes Tc-99m sulfur colloid, Tc-99m nanocolloid and Tc-99m macro-aggregated albumin (MAA) as they do not diffuse through peritoneal surfaces. These radiopharmaceuticals will stay below the diaphragm unless there is a connection such as pleural or scrotal communications (9).

Conclusion

In conclusion, peritoneal scintigraphy is useful for the evaluation of pleural effusion or hydrothorax in patient with continuous ambulatory peritoneal dialysis.

References:

1. Popovich RP, Moncrief JW, Nolph KD, Ghods AJ, Twardowski ZJ, Pyle W. Continuous ambulatory peritoneal dialysis. Annals of Internal Medicine. 1978;88(4):449-56.
2. Kopecky RT, Frymoyer PA, Witanowski LS, Thomas FD. Complications of continuous ambulatory peritoneal dialysis: diagnostic value of peritoneal scintigraphy. American Journal of Kidney Diseases. 1987;10(2):123-32.
3. Tokmak H, Mudun A, Türkmen C, Şanli Y, Cantez S, Bozfakioğlu S. The role of peritoneal scintigraphy in the detection of continuous ambulatory peritoneal dialysis complications. Renal failure. 2006;28(8):709-13.
4. Perez-Fontan M, Selgas R, Miguel J, Pardo M, González J, Conesa J, et al. Rupture of hernial sac as cause of massive subcutaneous dialysate leak in CAPD: diagnostic value of peritoneography. Dialysis & transplantation. 1986;15(2):74-7.
5. Nomoto Y, Suga T, Nakajima K, Sakai H, Osawa G, Ota K, et al. Acute hydrothorax in continuous ambulatory peritoneal dialysis–a collaborative study of 161 centers. American journal of nephrology. 1989;9(5):363-7.
6. Chow KM, Szeto CC, Li PKT, editors. Review Articles: Management Options for Hydrothorax Complicating Peritoneal Dialysis. Seminars in dialysis; 2003: Wiley Online Library.
7. Bae EH, Kim CS, Choi JS, Kim SW. Pleural effusion in a peritoneal dialysis patient. Chonnam medical journal. 2011;47(1):43-4.
8. Cho Y, D'Intini V, Ranganathan D. Acute hydrothorax complicating peritoneal dialysis: a case report. Journal of medical case reports. 2010;4(1):355.
9. Ziessman HA, O'Malley JP, Thrall JH. Nuclear Medicine: The Requisites E-Book: Elsevier Health Sciences; 2013.

ID #30: Ion beams for space radiation radiobiological effects studies

Ming Tsuey Chew[1], Andrew Nisbet[2,3], Masao Suzuki[4], Naruhiro Matsufuji[5], Takeshi Murakami[6], Bleddyn Jones[7], Mayeen Khandaker[1], David A Bradley[1, 2]

[1]Sunway University, School of Healthcare and Health Sciences, Centre for Biomedical Physics, No. 5, Jalan Universiti, Bandar Sunway, Selangor, Petaling Jaya, 47500 Selangor, Malaysia. [2]Department of Physics, Faculty of Engineering and Physical Sciences, University of Surrey, Guildford, GU2 7XH, UK. [3]The Department of Medical Physics, Royal Surrey County Hospital, Egerton Road, Guildford, GU2 7XX, UK. [4]Department of Basic Medical Sciences for Radiation Damages; National Institute of Radiological Sciences (NIRS), National Institutes for Quantum and Radiological Science and Technology, 4-9-1 Anagawa, Inage-ku, Chiba-shi, Chiba 263-8555, Japan. [5]Radiation Effect Research Team, Department of Accelerator and Medical Physics, NIRS, Japan. [6]Heavy-Ion Radiotherapy Promotion Unit & Department of Accelerator and Medical Physics, NIRS, Japan. [7]Gray Laboratory, CRUK/MRC Oxford Centre, Old Road Campus Research Building, Roosevelt Drive, University of Oxford, OX3 7DQ, UK.

Space radiation exposures to the heavier particles found in galactic cosmic rays (GCR) present a risk in manned space travel, most particularly to the central nervous system (CNS). GCR are made up of a mixture of multiple charged particles such as protons, ^{4}He and ^{56}Fe heavy ions. The most harmful to the CNS are the high charge and energy (HZE) particles, including ^{56}Fe because of its significant contribution to GCR dose and its high LET (Friedberg and Copeland, 2011). These HZE can result in altered cognitive function, reduced motor function and behavioural changes and long term chronic brain disease. For present interests, note is made of the lack of data on the biological response of ^{56}Fe ions. Ground based experiment can be used to infer the effects of the cosmic environment on cell survival, acknowledging that the response of tumour cells and healthy cells of other organs may be different thus limiting the accuracy of this inference. A mono-energetic beam of ^{56}Fe ions was generated by the Heavy Ion Medical Accelerator, National Institute of Radiological Sciences, Chiba. Present data refer to use of Glioblastoma multiforme (GBM) cells which, in arising from the brain, may infer the effects of space radiation on the CNS. Moreover, given that some strains of GBM cell lines are low dose hypersensitive, the very low doses that are used herein to study space radiation could be relevant. The limitation is that they are not normal cells; hence, restrictions need to be applied when interpreting these results.

Keywords: Space radiation, radiobiological effects, ^{56}Fe, galactic cosmic rays, GBM
Reference: Friedberg, W. and K. Copeland, *Ionizing Radiation in Earth's Atmosphere and in Space Near* Earth. 2011. 32.

Contact author: Chew Ming Tsuey; mtchew@sunway.edu.my

Acknowledgement: We thank the engineering staff of HIMAC for their support in making ion beam irradiations and acknowledge the technical support and assistance of Drs CH Liu, M Wada and N Autsavapromporn. This work was partly supported by the International Open Laboratory for the travel grants to NIRS/HIMAC, Japan to perform the experiments. This research was funded by PARTNER FP7-215840-2/Marie Curie and the ion beams were sponsored by NIRS/HIMAC, Chiba, Japan

ID #40: ^{68}Ga-Prostate-Specific Membrane Antigen (PSMA) PET/CT, a superior modality in restaging of prostate adenocarcinoma. A case report.

Muhammad Adib Abdul Onny[1], Mohd Fahmi Shukur Ramli[2], Lee Boon Nang[2], Hazlin Hashim[1]

[1]Nuclear Medicine Unit, Oncology & Radiological Sciences Cluster, Advanced Medical & Dental Institute, Universiti Sains Malaysia, Bertam, Pulau.Pinang, 13200, Malaysia. [2]Department of Nuclear Medicine, Institut Kanser Negara, Putrajaya, 62250, Malaysia.

Prostate adenocarcinoma is among the ten most common malignancy among male in Malaysia with incidence of 6.6 per 100000[1]. Prostate-Specific Membrane Antigen (PSMA) is a cell surface protein which is overly expressed in metastatic prostate lesions and coupling of positron emitting agent such as ^{68}Ga allows excellent imaging of these lesions. We present a case of a 75-year-old gentleman diagnosed with prostate adenocarcinoma, Gleason score 7(4+3). MRI pelvis showed bilateral local involvement with extracapsular extension and possible head of femur metastasis. However, bone scan was negative. He was started on anti-androgen therapy and a repeat bone scan after 3 years still showed no bone metastasis. However his serum PSA increased from 4.23ng/ml to 7.19ng/ml. ^{68}Ga-PSMA PET/CT was performed which eventually showed extensive local disease and extensive bone metastasis. Most of the PSMA positive bone lesions showed no significant CT changes. In light of the imaging findings, patient was started on IM Lucrin with prednisolone. ^{68}Ga-PSMA PET/CT has been shown to be sensitive in detecting metastatic lesion even in the setting of low PSA level. Various recent meta-analysis have shown that the sensitivity and specificity of ^{68}Ga-PSMA PET/CT are 61-80% and 84-97% respectively with another large review reported detection rate of 79.5% in the setting of biochemical recurrence[2,3,4]. This particular case has shown the benefit of ^{68}Ga-PSMA PET/CT in restaging of disease and assisting in the clinical management. In addition, the advent of theranostic approach allows ^{68}Ga-PSMA PET/CT to be paired with beta-emitting agents for the treatment of bone pain, an option that could be considered in this patient.

References

1. Azizah, Ab.M, Nor Saleha, I.T., Noor Hashimah, A., Asmah, Z.A., Mastulu, W. (2016). Malaysian National Cancer Registry Report 2007-2011.
2. Lenzo, N., Meyrick, D. and Turner, J. (2018). Review of Gallium-68 PSMA PET/CT Imaging in the Management of Prostate Cancer. *Diagnostics*, 8(1), p.16.
3. Perera, M., Papa, N., Christidis, D., Wetherell, D., Hofman, M., Murphy, D., Bolton, D. and Lawrentschuk, N. (2016). Sensitivity, Specificity, and Predictors of Positive 68 Ga– Prostate-specific Membrane Antigen Positron Emission Tomography in Advanced Prostate Cancer: A Systematic Review and Meta-analysis. *European Urology*, 70(6), pp.926-937.
4. Udovicich, C., Perera, M., Hofman, M., Siva, S., Del Rio, A., Murphy, D. and Lawrentschuk, N. (2017). 68 Ga-prostate-specific membrane antigen-positron emission tomography/computed tomography in advanced prostate cancer: Current state and future trends. *Prostate International*, 5(4), pp.125-129.
5. Evans, J., Jethwa, K., Ost, P., Williams, S., Kwon, E., Lowe, V. and Davis, B. (2018). Prostate cancer–specific PET radiotracers: A review on the clinical utility in recurrent disease. *Practical Radiation Oncology*, 8(1), pp.28-39.

Contact Author:
Muhammad Adib Bin Abdul Onny; roughnick12@gmail.com / dradib@student.usm.my

Acknowledgment

Our acknowledgment to the Director General of Health, Malaysia, Director of Institut Kanser Negara and Director of Advanced Medical & Dental Institute, Universiti Sains Malaysia.

Keywords

Prostate carcinoma, ^{68}Ga-PSMA PET/CT, Prostate-Specific Membrane Antigen, prostate-specific antigen, PET/CT, Theranostics.

ID #47: Comparison of standardized uptake value maximum (SUVmax) between metastastic and degenerative joint disease of the spine using bone scintigraphy with single photon emission computed tomography/ computed tomography (SPECT/CT) in prostate cancer

Mohd Fazrin Mohd Rohani[1,2], Hazlin Hashim[2], Syed Ejaz Shamim[1], Norazlina Mat Nawi[1], Wan Fatihah Wan Sohaimi[1]

[1]Nuclear Medicine, Radiotherapy and Oncology Department, Hospital Universiti Sains Malaysia, Kubang Kerian, Kelantan, 16150, Malaysia, *[2]Nuclear Medicine Unit, Oncological and Radiological Sciences Cluster, Advanced Medical and Dental Institute, Universiti Sains Malaysia, Bertam, Pulau Pinang, 13200, Malaysia*

Abstract: Qualitative interpretation in bone scan is often complicated by presence of degenerative joint disease (DJD) especially in the elderly (1,2). The aim of this study is to compare objectively ^{99m}Tc-methylene diphosphonate uptake between DJD and osseous metastases of the spine using semi-quantitative assessment with SPECT SUV (3). Bone scan with SPECT/CT using ^{99m}Tc-MDP were performed in 34 patients diagnosed with prostate carcinoma. SPECT/CT were performed based on our institutional standard guidelines (4). SUVmax based on body weight (5,6) of 238 normal vertebrae visualized in SPECT/CT were quantified as baseline. A total of 211 lesions in the spine were identified on bone scan. Lesions were characterized into DJD or bone metastases based on its morphology on low dose CT (7). Semi-quantitative evaluation using SUVmax were then performed on 89 DJD and 122 metastatic bone lesions. The mean SUVmax for normal vertebrae was 7.08 ± 1.97, 12.59 ± 9.01 for DJD and 36.64 ± 24.84 for bone metastases. The SUVmax of bone metastases were significantly greater than DJD (p value <0.05). To assess for diagnostic accuracy, receiver operating characteristics (ROC) curve was performed. The area under the curve (AUC) was found to be fairly high at 0.874 (95% CI: 0.826-0.921). The cut-off SUV value 19.04 gave a sensitivity of 73.8% and specificity of 85.4% in differentiating bone metastases from DJD. SPECT SUVmax was significantly higher in bone metastases than DJD. Semi-quantitative assessment with SUVmax can complement qualitative analysis. A cut-off SUVmax of 19.04 can be used to differentiate bone metastases from DJD.

References:

1. Gerard J O'Sullivan FLC, Carmel G Cronin. Imaging of bone metastasis: An update. World Journal of Radiology. 2015;7(8):202-11.
2. Saima Muzahir RJ, Glenn Liu, Lance T Hall, Alejandro Munoz Del Rio, Timothy Perk, Christine Jaskowiak, Scott B Perlman. Differentiation of metastatic vs degenerative joint disease using semi-quantitative analysis with ^{18}F-NaF PET/CT in castrate resistant prostate cancer patients. American Journal of Nuclear Medicine and Molecular Imaging. 2015;5(2):162-8.
3. Zafeirakis A. Scoring systems of quantitative bone scanning in prostate cancer: historical overview, current status and future perspectives. Hellenic Journal of Nuclear Medicine. 2014;17(2):136-44.
4. T. Van den Wyngaert KS, W. U. Kampen, T. Kuwert, W. van der Bruggen, H. K. Mohan, G. Gnanasegaran, R. Delgado-Bolton, W. A. Weber, M. Beheshti, W. Langsteger, F. Giammarile, F. M. Mottaghy, F. Paycha. The EANM practice guidelines for bone scintigraphy. European Journal of Nuclear Medicine and Molecular Imaging. 2016;43:1723-38.
5. Michal Cachovan AHV, Joachim Hornegger, Torsten Kuwert. Quantification of ^{99m}Tc-DPD concentration in the lumbar spine with SPECT/CT. European Journal of Nuclear Medicine and Molecular Imaging. 2013;3(45).
6. Tomohiro Kaneta MO, Hiromitsu Daisaki, Shintaro Nawata, Keisuke Yoshida, Tomio Inoue. SUV measurement of normal vertebrae using SPECT/CT with Tc-99m methylene diphosphonate. American Journal of Nuclear Medicine and Molecular Imaging. 2016;6(5):262-8.
7. Einat Even Sapir RHM, David C. Barnes, Christopher R. Pringle, Sian E. Iles, Michael J. Mitchell. Role of SPECT in differentiating malignant from benign lesions in the lower thoracic and lumbar vertebrae. Radiology. 1993;187(1):193-8.

Contact author: Mohd Fazrin Mohd Rohani; fazrinrohani@gmail.com

Acknowledgement: The authors would like to thank all the staff of Nuclear Medicine, Radiotherapy and Oncology Department, Hospital Universiti Sains Malaysia for their support and dedication.

Keywords: Bone scintigraphy, SPECT/CT, SPECT SUV, bone metastasis, prostate cancer, ^{99m}Tc-MDP

ID #56: Case Report - IORT in Pantai Hospital Kuala Lumpur

M.S.Ainina[1], Yong Qian Ying[1]

[1]*Pantai Hospital Kuala Lumpur, Bangsar, 59100, Malaysia*

Intraoperative Radiation Therapy (IORT) use low kV energy as it is done at tumour bed just after tumour was removed. IORT was introduced to treat breast, colon, spine and brain metastasis. There are two ways in using IORT for breast as it can be used alone (TARGIT-A) and act as a boost (TARGIT-B) that soon will be top up with external beam radiotherapy few weeks after done with the surgery. Pantai Hospital Kuala Lumpur (PHKL) already started with five cases of TARGIT-A IORT. It was successfully done by our OT team and physicist. Time taken for IORY procedure was depends on applicator size and dose prescribed by physicians. As dose prescribed by oncologist was 20Gy at 0mm from applicator surface, the irradiation time was controlled by applicator size only. Obviously, it took longer irradiation time for bigger applicator but for our presented case the biggest applicator size used was 4.5cm and the beam on time took less than 45 minutes.

Contact author: M.S.Ainina; ainina.safian@parkwaypantai.com

Keywords: Intraoperative Radiation Therapy, Breast cancer, TARGIT-A

ID #58: Bioactive glass: exploring its potentials use for treatments based on *in vivo* and *in vitro* studies

Haruna S. J[1], Shahrul H[1] and Fazliah SNMN[2]

[1]Oncological & Radiological Sciences Cluster, Advanced Medical and Dental Institute, Universiti Sains Malaysia, 13200 Kepala Batas, Penang, Malaysia; [2]Craniofacial & Biomaterials Sciences Cluster, Advanced Medical and Dental Institute, Universiti Sains Malaysia, 13200 Kepala Batas, Penang, Malaysia

Biomaterials received intense research interest over the last decade. One of the biomaterials that is extensively studied is the bioactive glass (BG). This paper aims to highlight various methods adopted to produce the BG, their characterisation and potential application in medical and dental fields. Systematic review based on BG as keyword retrieved from databases highlighted that manufacturing techniques commonly used to produce BG include melt-derived, melt-annealed, freeze-casting and sol-gel methods. BG composition was modified based on the gold standard 45S5® BG SiO2-CaO-NaO-P2O5 system by addition of different types of alkaline earth metal such as strontium, magnesium, zinc, cobalt and many others where each of these ions possessed specific function to aid bone regeneration, enzymatic function, antibacterial, healing and angiogenesis. BG exists as powder, pellet, tablets and three-dimensional (3D) structures with the addition of other polymeric materials such as gelatin, polycaprolactone, polylactic acid for enhanced mechanical and physical properties. Besides that, bioactive glass-based scaffolds can be further functionalised to achieve higher mechanical stability, particularly toughness, and to provide drug-delivery capability. In addition, synthetic and natural polymer-coatings are used to increase mechanical stability and serve as carrier matrix for the local release of growth factors or antibiotics to support bone tissue formation. BG has shown numerous biocompatibility capabilities towards various types of cells *in vitro* while i*n vivo* studies showed no adverse effect and BG exhibited high angiogenesis which facilitate tissue repair. Taken together, bioactive glass displays high biocompatibility which show that it has potential to be explored further for medical and dental applications.

Contact author: fazliah@usm.my

Presenting author: Haruna S Jallow

Email of presenting author: harunajallow00@gmail.com

Keywords: bioactive glass, biomaterials, bone formation

Cancer Cell Biology

ID #8: Prenatal Ultrasound Induces Apoptotic Neurons and Glial Cells (AC) in Rabbit Fetal Brain: A Biochemical analysis

F. W. A. Zaiki[1], S. M. Dom[2]

[1]Kulliyyah of Allied Health Sciences, International Islamic University Malaysia, Kuantan, Pahang, 25200, Malaysia, [2] Faculty of Health Sciences, Universiti Teknologi MARA, Puncak Alam, Selangor, 42300, Malaysia.

Ultrasound wave propagates through tissues are absorbed and converted to heat. Findings in numerous studies utilizing the ultrasound exposure have also convinced the existence of ultrasound-induced apoptosis in the exposed cells. Hence, this current study was aimed to detect the apoptotic neurons and glial cells (AC) in the rabbit fetal brain resulting from the prenatal ultrasound exposure. The terminal dUTP nick end-labeling (TUNEL) assay staining by ApopTag® Plus Peroxidase In-Situ Apoptosis Detection Kit (S7101) from Millipore, USA was used. The effects of prenatal ultrasound to neurons and glial cells were analyzed by comparing the AC counts in the rabbit fetal cerebral cross section between the expose and control groups. At least 3 TUNEL stained slides were randomly examined from each subject making a total of N=102 (30 minutes exposure, n= 9; 60 minutes exposure, n= 9; 90 minutes exposure, n= 9; control, n= 7). The temperature increment was measured during the prenatal ultrasound exposure, which the maximum was 1.0, 1.8 and 3.3°C for 30, 60 and 90 minutes of exposure, respectively. Data was analyzed using SPSS version 21.0. The p-values were significant at all stages of gestation with all the p-values were less than 0.001 ($p<0.001$). The results suggested that there were significant differences in AC counts in all stages of gestation between groups of different exposure duration. The detection of the DNA fragmentation in TUNEL positive cell could serve as an evidence in suggesting the apoptosis was induced by the ultrasound exposure.

Contact author: F. W. A. Zaiki; farahzaiki@iium.edu.my

Acknowledgement: The authors would like to acknowledge the Research Management Centre of International Islamic University Malaysia, Malaysia for the Research Initiative grant Scheme (RIGS) grant awarded (RIGS 16-300-0464) and Research Management Institute (RMI) of Universiti Teknologi MARA, Malaysia for the Research Intensive Faculty (RIF) grant awarded (600-RMI/DANA/5/3/RIF (229/2012).

Keywords: prenatal, ultrasound, apoptotic, neuron, glial, rabbit, fetal, brain, biochemical, TUNEL.

ID #13: HDR brachytherapy in reirradiation of local nasopharyngealrecurrence

Mohamed Ait erraisse[1], Wissal Hassani[1], Moulay Ali Youssoufi[2], Khalid Hassouni[1]

[1]Department of Radiotherapy, University Hospital Hassan II, Fes, 30003, Morocco; [2] Faculty of Sciences (LPHE, M-S), University Mohammed V, Rabat, 10010, Morocco;

Purpose: Nasopharyngeal carcinoma (NPC) is the most frequent cancer of head and neck in North Africa and South East Asia. Reirradiation of local recurrence is limited by the dose constraints. Brachytherapy alone or in combination with EBRT can be a good compromise. The aim of this study was to determine the role of brachytherapy in safety reirradiation of recurrent NPC. Material and Methods: This is a retrospective study of 8 patients with nasopharyngeal cancer recurrence collected in the radiotherapy department of the University hospital Hassan II in Fez between January 2014 and December 2017. Results: The average age of our patients is 42 years old. the average time to onset of relapse is 29 months. All patients received external radiation therapy at 70 Gy on macroscopic tumor volume (tumor and lymphadenopathy) during initial irradiation with or without chemotherapy. relapse was localized in 5 patients and associated with lymph node involvement in 3 patients. 2 patients received exclusive high-dose-rate brachytherapy and 6 received external radiation radiotherapy followed by brachytherapy. The total radiation dose EQD2 was 60 to 66 Gy. With an average follow-up of 20 months, 37.5% of patients are alive and in complete remission. Conclusion: Brachytherapy alone or after EBRT could play an important role in reirradiation of locally recurrent NPC with acceptable toxicity.

Contact author: Mohamed Ait Erraisse; aiterraissemohamed@gmail.com

Keywords: nasopharynx, brachytherapy, reirradiation

ID#25: Cytotoxic Effects of Low-Level Laser Irradiation on Human Breast Cancer MCF-7 Cells: *In Vitro* Study

Husna Azdiyah Habita @ Habit[1], Nursakinah Suardi[1], Shahrom Mahmud[1], Rabiatul Basria S.M.N Mydin[2], Siti Khadijah Mohd Bakhori[1]

[1]School of Physics, Universiti Sains Malaysia, Pulau Pinang, 11800, Malaysia; [2]Oncological and Radiological Sciences Cluster, Advanced Medical and Dental Institute, Universiti Sains Malaysia, Penang, 13200, Malaysia

Today, it was realized that laser therapy had the potential to replace the recent cancer treatments such as chemotherapy and radiotherapy as they have high potential to damage surrounding healthy cells although they are proven to be effective in reducing the size of tumours. This study focusing on low level laser therapy which is selectively kill cancer cells, as the light beam can directly expose to the targeted site while not affecting the normal cells. It is non-invasive due its energy densities are lower than other types of laser. The MCF-7 cells were plated to a density of 4×10^4 cells/well in 96-well plate and incubated for 24h. Then, the cells were treated with 532 nm laser at different power and dose. In Group 1, the laser power was 1 mW with different doses of 0.24 J cm^{-2} , 0.72 J cm^{-2} , and 1.2 J cm^{-2} while the Group 2, the laser power was 15 mW with different dose of 3.6 J cm^{-2} , 10.8 J cm^{-2} , and 18 J cm^{-2} . In Group 3, the MCF-7 will be treated with 30 mW at doses of 7.2 J cm^{-2} , 21.6 J cm^{-2} and 36 J cm^{-2} . After that, the absorbance of treated MCF-7 cells were measured by Alamar Blue to determine the toxicity of laser exposure on the cells. 1 mW laser irradiation proved to be less efficient at lowest dose of 0.24 J cm^{-2} when the cell inhibits only 21 %. The cell viability reduced to 90 % after treated with the same power as the dose increases whereas the cells completely killed after treated with 15 mW and 30 mW. This study highlights the LLLT could become a promising therapy by providing localized therapies and improve patient quality of life.

Contact author: Husna Azdiyah Binti Habita @ Habit; husnaazdiyah24@gmail.com, Nursakinah Suardi; nsakinahsuardi@usm.my

Acknowledgement: The authors would like to thank Universiti Sains Malaysia (USM), Penang for the grant provided (203/PFIZIK/6711598), the staff of Oncology and Radiological Cluster, Advanced Medical and Dental Institute (AMDI) for their assistance and support of this research.

Keywords: Laser, AuNPs, MCF-7 cell line

ID #36: Specific inhibition of miR130a using CRISPR/Cas9 induces the proliferation and migration of non-small cell lung cancer cell line.

Siti Razila Abdul Razak[1], Nur Ainina Abdollah[1], Nabil Izzatie Mohamad Safiai[1], Muhammad Khairi Ahmad[1], Kumitaa Theva Das[2]

[1]*Oncological and Radiological Sciences Cluster, Advanced Medical and Dental Institute, Kepala Batas, Pulau Pinang, 13200, Malaysia;* [2]*Infectomics Cluster, Advanced Medical and Dental Institute, Kepala Batas, Pulau Pinang, 13200, Malaysia.*

Molecular alterations of microRNA (miRNA) such as miR130a, are frequently observed in regulation of many types of cancers, including the non-small cell lung cancer (NSCLC). However, the specific roles of miR130a in NSCLC has been poorly studied. In this study, we utilized a genome editing tool, clustered regularly interspaced short palindromic repeat (CRISPR)-Cas9, to identify specific target sites for the knockdown of miR130a. We further investigated the effects of the suppression in A549 NSCLC cell line to better understand the significance of miR130a in NSCLC. Briefly, 20 bp single-guided RNA sequences that targeted the stem loop, 3' and 5' sites of miR130a gene were cloned into lentiCRISPRv2. The cloned plasmids were transfected into A549 cell line and selection was performed using puromycin. Total RNA was extracted and mature level of miR130a-3p and miR130a-5p were quantified with real-time PCR. Proliferation and migration assays were also conducted. Our results showed that the CRISPR/Cas9 that targeted the 3' site and stem loop of miR130a gene were able to significantly down-regulate the endogenous expression of mature miR130a-3p and 5p by two and three-fold respectively. No changes were observed when Cas9 targeted the 5' site of the miR130a gene. The growth and migrations assays correlated with our real-time PCR analysis, in which suppression of miR130a-3p significantly increased the growth and migration of A549 cells. No significant changes were observed in cells with suppressed expression of miR130a-5p. Our encouraging results highlight the efficacy and specificity of CRISPR-Cas9 to knockdown miR130a, and suggest that inhibition of miR-130a-3p could play an important role in the regulation of NSCLC cancer.

Contact author: Siti Razila Abdul Razak, sitirazila@usm.my

Acknowledgement: This project is supported by USM Short Term Grant (304/CIPPT/6313203) and Fundamental Research Grant Scheme (203/CIPPT/6711505)

Keywords: miR130a, non-small cell lung cancer, A459 proliferation, A549 scratch assay, A549 migration assay

ID #39: Construction of Yeast Two-Hybrid (Y2H) Bait Vector for Screening of Selected Deubiquitinases (DUBs)-interacting Protein.

Nur Wahida Zulkifli[1] and Nurulisa Zulkifle[1]

[1]*Oncological and Radiological Sciences Cluster, Advanced Medical & Dental Institute, Universiti Sains Malaysia, Kepala Batas, Penang, 13200, Malaysia*

Over the past few years, deubiquitinases (DUBs) has emerged as promising new therapeutic targets in many diseases including cancer. Defining DUBs interaction landscape is very important in order to understand DUBs mechanism. Yeast two-hybrid (Y2H) is a yeast-based genetic assay that is commonly used to detect novel protein-protein interaction. In this work, Y2H bait vectors were constructed for screening of selected DUBs-interacting proteins. Total RNA was extracted from Human Embryonic Kidney (HEK293) cell line by using TRIzol. mRNA was isolated using Oligotex mRNA Mini Kit and cDNA library was constructed. Selected DUBs (e.g. OTUB1, OTUB2, and OTULIN) genes were amplified using *Taq* 2X Master Mix to produce PCR products of selected DUBs genes with dA overhangs at the 3'-end. The selected DUBs genes were directly ligated into the pCR 8/GW/TOPO vector using pCR 8/GW/TOPO TA Cloning Kit to get the entry clone. Then the recombinant TOPO-DUBs plasmids entry clones were transformed into NEB 5-α Competent *E.coli* cells and recombinant plasmids were purified by using QIAGEN Plasmid Mini Kit. The recombinant TOPO-DUBs plasmids were confirmed by colony PCR and DNA sequencing. LR recombination reaction was performed between recombinant TOPO-DUBs plasmid entry clone and pDEST32 yeast expression vector using Gateway LR Clonase II Enzyme Mix. The bait plasmids of pDEST32-DUBs were validated by colony PCR and DNA sequencing. Results showed that the selected DUBs were successfully cloned into pDEST32 vector and ready to be transfected into *Saccharomyces cerevisiae* strain MaV203. Currently, construction of Y2H prey vector using cDNA library are in progress. Upon completing the cDNA prey vector, the Y2H GAL4 system can be utilized to find selected DUBs-interacting proteins.

Contact author: Nur Wahida Zulkifli; ishida91_ida@yahoo.com

Acknowledgement: This work is supported by the Government of Malaysia under grant FRGS/1/2014/SG05/USM/02/1. The scholarships to Nur Wahida Zulkifli are funded by MyBrain15 KPT.

Keywords: Yeast Two-Hybrid (Y2H), Bait vector, Deubiquitinases (DUBs)

ID #41: Generation of Indels for dual-specificity phosphatase 6 (DUSP6) gene suppression in colorectal cancer cell line via CRISPR-Cas9 system.

[1]Muhammad Khairi Ahmad, [1]Nur Ainina Abdollah, [2]Kumitaa Theva Das, [1]Siti Razila Abdul Razak

[1]Oncological & Radiological Sciences Cluster, Advanced Medical & Dental Institute, Universiti Sains Malaysia, Bertam, 13200 Kepala Batas, Pulau Pinang, Malaysia, [2]Infectomics Cluster, Advanced Medical & Dental Institute, Universiti Sains Malaysia, Bertam, 13200 Kepala Batas, Pulau Pinang, Malaysia.

Dual-specificity phosphatase 6 (DUSP6) plays vital role as pro-oncogenic or tumour-suppressor in various types of cancers. It interacts with ERK1/2 via negative feedback regulation in MAPK pathway, which aberration is frequently observed in cancers. However, the specific role of DUSP6 in colorectal cancer (CRC) is poorly studied. Gene-editing system has long been used to study gene and carcinogenic pathway in cancer. However, the cost, time and practicality to design and establish the system to manipulate gene expression could limit the experimental process. The emergence of CRISPR-Cas9 system with reportedly elegant features including cost -saving, target -design simplicity, robustness and efficiency would help researchers to investigate many cancers. In this study, lentiCRISPRv2-Cas9 mediated system was employed to generate indels for DUSP6 gene suppression in HT-29 CRC cell line. The DUSP6 site-specific guide RNAs (gRNAs) were designed using CRISPR design tool (http://crispr.mit.edu/) and cloned into lentiCRISPRv2 plasmid. The lentiCRISPRv2-DUSP6 was then transfected into HT-29 cell line using Lipofectamine 3000, incubated for three days, and the successfully transfected cells were selected for four days using puromycin. The genomic DNA was extracted from the transfected cells, and was analysed using GeneArt genomic cleavage detection assay. The assay shows the presence of three separated bands which marked successful generation of indels in DUSP6 gene in HT-29 cell line that would expectedly disrupt its reading frame causing gene suppression. However, further analysis of the gene suppression can be confirmed by real-time PCR and western-blot. Thus, our study suggests lentiCRISPRv2-mediated system can be successfully used to generate indels in DUSP6 gene for gene suppression in HT-29 CRC cell line.

Contact author: Muhammad Khairi Ahmad; m.khairi_tpm@yahoo.com

Acknowledgement: This work was funded by a grant from Fundamental Research Grant Scheme, Ministry of Higher Education Malaysia (Grant No. 203.CIPPT.6711505).

***Keywords**: Colorectal cancer; DUSP6; lentiCRISPRv2-Cas9; Indels*

ID #61: Roles of lipids in development of anticancer drug resistance in MCF7 cells

Auni Fatin Abdul Hamid[1], Shahrul Bariyah Sahul Hamid[1]

[1]*Oncological and Radiological Sciences Cluster, Advanced Medical and Dental Institute, Universiti Sains Malaysia, Penang, 13200, Malaysia*

Breast cancer is the most common type of cancer among women world wide and it is the leading cause of death among women in Malaysia. Clinical data have indicated that oxidized low density lipoprotein (oxLDL) and very low density lipoprotein (VLDL) are involved in breast cancer progression. Despite the current advancement in technologies, drug resistance remains as a major obstacle in delivering effective breast cancer treatment. Therefore, this study aims to investigate the role of lipids in development of resistance to anticancer drugs. Tamoxifen-resistant MCF7 (Tam-R) was developed by pulse treatment method. The cells were exposed to gradual increase of tamoxifen concentration from 1 to 5 μM for 3 days in Dulbecco's Modified Eagle's medium (DMEM) without phenol red. This was followed by cell viability test to determine the fold-resistance of tamoxifen-treated cells relative to the parent MCF7 cells. It was done at concentration of tamoxifen between 0 to 100 μM. Further analysis was carried out through wound-healing assay. Two-hundred microliter tips were used to make a "wound" at the center of the well. Then, the cells were treated with 10 μg/mL of oxLDL and images were taken at 0 hour and 72 hour for comparison. From the cell viability test, results indicated that the Tam-R cells had 2-fold resistance which is considered as a clinically relevant drug-resistant cancer cell line model. After 72 hours of oxLDL treatment, both parent MCF7 and Tam-R cells showed higher percentage of wound closure compared to control. Tam-R cells had 34 % of wound closure, whereas parent MCF7 cells had 21 % of wound closure. This data suggests that oxLDL promotes cell migration in breast cancer cells and may play important role in increasing resistance against tamoxifen.

Contact author: Auni Fatin Abdul Hamid; aunifatinhamid@yahoo.com

Acknowledgement: This study was funded by Fundamental Research Grant Scheme (FRGS)

Keywords: oxidized-low density lipoprotein, drug resistant, breast cancer